

1 **Exploring the impacts of unprecedented climate extremes on forest ecosystems: hypotheses**
2 **to guide modeling and experimental studies**

3

4 Jennifer A. Holm^{1,*}, David M. Medvigy², Benjamin Smith^{3,4}, Jeffrey S. Dukes⁵, Claus Beier⁶,
5 Mikhail Mishurov³, Xiangtao Xu⁷, Jeremy W. Lichstein⁸, Craig D. Allen⁹, Klaus S. Larsen⁶, Yiqi
6 Luo¹⁰, Cari Ficken¹¹, William T. Pockman¹², William R.L. Anderegg¹³, and Anja Rammig¹⁴

7

8 ¹ Lawrence Berkeley National Laboratory, Berkeley, California, USA

9 ² University of Notre Dame, Notre Dame, Indiana, USA

10 ³ Dept of Physical Geography and Ecosystem Science, Lund University, Lund, Sweden

11 ⁴ Hawkesbury Institute for the Environment, Western Sydney University, Penrith, NSW 2751,
12 Australia

13 ⁵ Department of Forestry and Natural Resources and Biological Sciences, Purdue University,
14 West Lafayette, Indiana, USA

15 ⁶ Department of Geosciences and Natural Resource Management, University of Copenhagen,
16 Frederiksberg, Denmark

17 ⁷ Department of Ecology and Evolutionary Biology, Cornell University, Ithaca, New York, USA

18 ⁸ Department of Biology, University of Florida, Gainesville, Florida, USA

19 ⁹ U.S. Geological Survey, Fort Collins Science Center, New Mexico Landscapes Field Station,
20 Los Alamos, New Mexico, USA

21 ¹⁰ Center for Ecosystem Science and Society, Department of Biological Sciences, Northern
22 Arizona University, Flagstaff, Arizona, USA

23 ¹¹ Department of Biology, University of Waterloo, Waterloo, Ontario, Canada

24 ¹² Department of Biology, University of New Mexico, Albuquerque, New Mexico, USA

25 ¹³ School of Biological Sciences, University of Utah, Salt Lake City, Utah, USA

26 ¹⁴ Technical University of Munich, TUM School of Life Sciences Weihenstephan, Freising,
27 Germany

28

29 * *Correspondence to:* Jennifer Holm; 510-495-8083; jaholm@lbl.gov

30

31 **Keywords:** demographic modeling; mortality; drought; recovery; carbon cycle; nonstructural
32 carbohydrate storage; plant hydraulics; dynamic vegetation

33

34 **Abstract**

35

36 Climatic extreme events are expected to occur more frequently in the future, increasing the
37 likelihood of unprecedented climate extremes (UCEs), or record-breaking events. UCEs, such as
38 extreme heatwaves and droughts, substantially affect ecosystem stability and carbon cycling by
39 increasing plant mortality and delaying ecosystem recovery. Quantitative knowledge of such
40 effects is limited due to the paucity of experiments focusing on extreme climatic events beyond
41 the range of historical experience. Here, we present a road map of how two dynamic vegetation
42 demographic models (VDMs) can be used to investigate hypotheses surrounding ecosystem
43 responses to UCEs (e.g., unprecedented droughts). As a result of nonlinear ecosystem responses
44 to UCEs, that are qualitatively different from responses to milder extremes, we consider both
45 biomass loss and recovery rates over time, by reporting a time-integrated carbon loss as a result
46 of UCE, relative to the absence of drought. Additionally, we explore how unprecedented
47 droughts in combination with increasing atmospheric CO₂ and/or temperature may affect
48 ecosystem stability and carbon cycling. We explored these questions using simulations of pre-
49 drought and post-drought conditions at well-studied forest sites, using the ED2 and LPJ-GUESS
50 models. Due to the two models having different but plausible representations of processes and
51 interactions, they diverge in sensitivity of nonlinear biomass loss due to drought duration or
52 intensity, and differ between each site. Biomass losses are most sensitive to drought duration in
53 ED2, but to drought intensity in LPJ-GUESS. Elevated atmospheric CO₂ concentrations (eCO₂)
54 alone did not completely buffer the ecosystems from carbon losses during UCEs in the majority
55 of our simulations. Our findings highlight contrasting differences in process formulations and
56 uncertainties in models, most notably related to availability in plant carbohydrate storage and the
57 diversity of plant hydraulic schemes, in projecting potential ecosystem responses to UCEs. We
58 provide a summary of the current state and role of many model processes that give way to
59 different underlying hypotheses of plant responses to UCEs, reflecting knowledge gaps, which
60 should be tested with targeted field experiments and an iterative modeling-experimental
61 conceptual framework.

62 **1 Introduction**

63 The increase in extreme climate and weather events, such as prolonged heatwaves and
64 droughts as seen over the last three decades, are expected to continue to increase in frequency
65 and magnitude, leading to progressively longer and warmer droughts on land (IPCC 2012, 2021).
66 Droughts are affecting all areas of the globe, more than any other natural disturbance, and recent
67 droughts have broken long-standing records (Ciais et al., 2005; Phillips et al., 2009; Williams et
68 al., 2012; Matusick et al., 2013; Griffin and Anchukaitis, 2014; Asner et al., 2016; Feldpausch et
69 al., 2016; Seneviratne et al., 2021). Such ‘unprecedented climate extremes’ (UCEs; “record-
70 breaking events”, IPCC (2012)) that are larger in extent and longer-lasting than historical norms
71 can have dramatic consequences for terrestrial ecosystem processes, including carbon uptake and
72 storage and other ecosystem services (Reichstein et al., 2013; Settele, 2014; Allen et al., 2015;
73 Brando et al., 2019; Kannenberg et al., 2020). Thus, to better anticipate the implications of
74 climatic changes for the terrestrial carbon sink and other ecosystem services, we need to better
75 understand how ecosystems respond to extreme droughts and other UCEs.

76 To learn how ecosystems respond to rarely experienced or unprecedented conditions,
77 ecologists can experimentally manipulate environmental conditions (Rustad, 2008; Beier et al.,
78 2012; Meir et al., 2015; Aguirre et al., 2021). However, the majority of such experiments apply
79 moderate treatments based on a historical sense, which are mostly weaker in intensity and/or
80 shorter in duration than potential future UCEs (Beier et al., 2012; Kayler et al., 2015; but see Luo
81 et al., 2017), and single experiments have low power to detect effects of stressors on ecosystem
82 responses (Yang et al., 2022). Additionally, most experiments examine low-stature ecosystems,
83 such as grassland, shrubland or tundra, due to lower requirements for infrastructure and financial
84 investment compared to mature forests. However, forests may respond qualitatively differently
85 to UCEs than other ecosystems, in part due to mortality of large trees and strong nonlinear
86 ecosystem responses, with long-lasting consequences for ecosystem-climate feedbacks (Williams
87 et al., 2014; Meir et al., 2015). Ecosystem responses to naturally occurring extreme droughts and
88 heatwaves have been documented (Ciais et al., 2005; Breshears et al., 2009; Feldpausch et al.,
89 2016; Matusick et al., 2016; Ruthrof et al., 2018; Powers et al., 2020); however, these rapidly-
90 mobilized post-hoc studies often are unable to measure all critical variables and may lack
91 consistently collected data for comparison with pre-drought conditions, thus limiting their
92 inferential power and ability to improve quantitative models. The difficulties of performing

93 controlled real-world experiments of UCEs at broad spatial and temporal scales make process-
94 based modeling a valuable tool for studying potential ecosystem responses to extreme events.

95 Process-based models can be used to explore potential ecosystem impacts using projected
96 climate change over broad spatial and temporal scales (Gerten et al., 2008; Luo et al., 2008;
97 Zscheischler et al., 2014; Sippel et al., 2016), as seen in a few modeling studies that have
98 synthesized and improved our process-level understanding of UCE effects (McDowell et al.,
99 2013; Dietze and Matthes, 2014). However, due to the overly simplified representation of
100 ecological processes in most land surface models (LSMs) – the terrestrial components of Earth
101 System Models (ESMs) used for climate projections – it is doubtful whether most of these
102 models adequately capture ecosystem feedbacks and other responses to UCEs (Fisher and
103 Koven, 2020). For example, only a few ESMs in recent coupled model intercomparison projects
104 (CMIP6) and IPCC climate assessments (Ciais et al., 2013; Arora et al., 2020) include vegetation
105 demographics (Döscher et al., 2022), and most rely on prescribed, static maps of plant functional
106 types (PFTs) (Ahlström et al., 2012). Other LSMs simulate PFT shifts (i.e., dynamic global
107 vegetation models, DGVMs; Sitch et al., (2008)) based on bioclimatic limits, instead of
108 emerging from the physiology- and competition-based demographic rates that determine
109 resource competition and plant distributions in real ecosystems (Fisher et al., 2018). Although a
110 new generation of LSMs with more explicit ecological dynamics and structured demography is
111 emerging (Holm et al., 2020; Koven et al., 2020; Döscher et al., 2022), most current ESMs are
112 limited in ecological detail and realism (e.g., ecosystem structure, demography, and
113 disturbances). Failing to mechanistically represent mortality, recruitment, and disturbance – each
114 of which influences biomass turnover and carbon (C) allocation (Friend et al., 2014) – limits the
115 ability of these models to realistically forecast ecosystem responses to anomalous environmental
116 conditions like UCEs (Fisher et al., 2018).

117 Evaluating and improving the representation of physiological and ecological processes in
118 ecosystem models is critical for reducing model uncertainties when projecting the effects of
119 UCEs on long-term ecosystem dynamics and functioning. Vegetation demography, plant
120 hydraulics, enhanced representations of plant trait variation, explicit treatments of resource
121 competition (e.g., height-structured competition for light), and representing major disturbances
122 (e.g., extreme drought) have all been identified as critical areas for advancing current models
123 (Scheiter et al., 2013; Fisher et al., 2015; Weng et al., 2015; Choat et al., 2018; Fisher et al.,

124 2018; Blyth et al., 2021) and are necessary advances for realistically representing the ecosystem
125 impacts of UCEs. In this perspectives focused paper we look at the differences in these
126 processes, and how they contribute to uncertainty across multiple temporal phases surrounding
127 an extreme event: predicting an ecosystem's pre-disturbance resistance, which influences the
128 degree of impact and recovery from UCEs. Table 1 describes a summary of model mechanisms
129 that affect pre-drought resistance and post-drought recovery and we suggest are critical areas
130 further research (ca. Frank et al., 2015).

131 In order to inform our discussion, we explore the potential responses of forest ecosystems
132 to UCEs using two state-of-the-art process-based demographic models (vegetation demographic
133 models, VDMs; Fisher et al., (2018)), a unique model exploration-discussion approach to help
134 highlight new paths forward for model advancement. We first present conceptual frameworks
135 and hypotheses on potential ecosystem responses to UCEs based on current knowledge. We then
136 present VDM simulations for a range of hypothetical UCE scenarios to illustrate current state-of-
137 the-art model representations of eco-physiological mechanisms expected to drive responses to
138 UCEs. While a variety of UCE-linked biophysical tree disturbance processes (e.g., fire, wind,
139 insect outbreaks) can drive nonlinear ecosystem responses, we focus specifically on extreme
140 droughts, which have important impacts on many ecosystems around the world (e.g. Frank et al.,
141 2015, IPCC 2021). By studying modeled responses to UCEs, we explore the limits to our current
142 understanding of ecosystem responses to extreme droughts and their corresponding thresholds
143 and tipping points. As anthropogenic forcing has increased the frequency, duration, and intensity
144 of droughts throughout the world (Chiang et al., 2021), we explore how eCO₂ and rising
145 temperatures may affect drought-induced C loss and recovery trajectories, and how the scientific
146 community can iteratively address these questions through experiments and modeling studies.
147 We believe the combination of using cutting-edge VDMs alongside an inspection of current gaps
148 in knowledge will help guide modeling and experimental advances in order to address novel
149 forest responses to climate extremes.

150

151 **1.1 Conceptual and Modeling Framework for Hypothesis Testing:**

152 We combine conceptual frameworks (Fig. 1) and ecosystem modeling to test two
153 hypotheses on potential responses of plant carbon stocks to UCEs. The first hypothesis is:

154 ***Hypothesis (H1). Terrestrial ecosystem responses to UCEs will differ qualitatively from***
155 ***ecosystem responses to milder extremes because responses are nonlinear. Nonlinearities can***
156 ***arise from multiple mechanisms – including shifts in plant hydraulics, C allocation,***
157 ***phenology, and stand demography – and can vary depending on the pre-drought state of the***
158 ***ecosystem.***

159 We present four conceptual relationships that describe terrestrial ecosystem responses to varying
160 degrees of extreme events (Fig. 1). Change in vegetation C stock is related to drought intensity
161 and/or drought duration in a near-linear relationship (Fig. 1a, H0, null hypothesis), which has
162 some observational support from annual and perennial grassland ecosystems, shrublands and
163 savannas across the globe (Bai et al., 2008; Muldavin et al., 2008; Ruppert et al., 2015). We
164 recognize that most ecological systems are nonlinear, thus alternatives to the null hypothesis are
165 that biomass loss increases nonlinearly with increased drought intensity (i.e., reduction in
166 precipitation) represented by a threshold-based relationship (Fig. 1a, H1a), increased drought
167 duration (i.e., prolonged drought with the same intensity) by shifting the near-linear relationship
168 downwards via increasing slopes (Fig. 1a, H1b), or the combination of both intensity and
169 duration (Fig. 1a, H1c). These hypotheses are supported by observations from the Amazon Basin
170 and Borneo (Phillips et al., 2010) where tree mortality rates increased nonlinearly with drought
171 intensity. Similarly, plant hydraulic theories predict nonlinear damage to the plant-water
172 transport systems, and thus mortality risk, as a function of drought stress (Sperry and Love,
173 2015). In particular, longer droughts are more likely to lead to lower soil water potentials,
174 leading to a nonlinear xylem damage function even if stomata effectively limit water loss (Sperry
175 et al., 2016).

176 ***Hypothesis (H2): The effects of increasing atmospheric CO₂ concentration (eCO₂) will***
177 ***alleviate impacts of extreme drought stress through an increase in vegetation productivity and***
178 ***water-use efficiency, but only up to a threshold of drought severity, while increased***
179 ***temperature (and related water stress) will exacerbate tree mortality.***

180 This second hypothesis is based on growing evidence that effects of eCO₂ and climate
181 warming may interact with effects of drought intensity on ecosystems. The CO₂ fertilization
182 effect enhances vegetation productivity (e.g., net primary production, NPP) (Ainsworth and
183 Long, 2005; Norby et al., 2005; Wang et al., 2012), but this fertilization effect is generally

184 reduced by drought (Hovenden et al., 2014; Reich et al., 2014; Gray et al., 2016). Drought events
185 often coincide with increased temperature, which intensifies the impact of drought on
186 ecosystems (Allen et al., 2015; Liu et al., 2017), resulting in nonlinear responses in mortality
187 rates (Adams et al., 2009; Adams et al., 2017a). The evaluation of C cycling in VDMs with
188 doubling of CO₂ (only “beta effect”) showed a large carbon sink in a tropical forest (Holm et al.,
189 2020), but the inclusion of climate interactions in VDMs needs to be further explored.

190 Here, we relate ecosystem responses to UCEs by calculating the “integrated carbon (C)
191 loss” (Fig. 1b and see Methods), which integrates C loss from the beginning of the drought until
192 the time when C stocks have recovered to 50% of the pre-drought level. In response to drought,
193 warming, and eCO₂, divergent potential C responses (gains and losses; Fig. 1c) can be expected
194 (Keenan et al., 2013; Zhu et al., 2016; Adams et al., 2017a). For example, a grassland
195 macrocosm experiment found that eCO₂ completely compensated for the negative impact of
196 extreme drought on net carbon uptake due to increased root growth and plant nitrogen uptake,
197 and led to enhanced post-drought recovery (Roy et al., 2016). However, a 16-year grassland
198 FACE and the SoyFACE experiments showed that CO₂ fertilization effects were reduced or
199 eliminated under hotter/drier conditions (Gray et al., 2016; Obermeier et al., 2016). Reich et al.,
200 (2014) also found that CO₂ fertilization effects were reduced in a perennial grassland by water
201 and nitrogen limitation.

202 A corollary to our H2 is that conditions that favor productivity (e.g., longer growing
203 seasons and/or CO₂ fertilization) will enhance vegetation growth leading to “structural
204 overshoot” (SO; Fig. 1d; adapted from and supported by Jump et al., 2017), and can amplify the
205 effects of UCEs. Enhanced vegetation growth coupled with environmental variability can lead to
206 exceptionally high plant-water-demand during extreme drought and water stress, resulting in a
207 “mortality overshoot” (MO; Fig 1d). We conceptualize how oscillations between SO and
208 associated MO could be amplified by increasing climatic variability and UCEs (Fig. 1d).
209 Confidence is low as to how historically unprecedented eCO₂ levels and temperatures will affect
210 ecosystems in the future (i.e., the widening of the shaded areas compared to historical, Fig. 1d).
211 We expect, however that a rapidly changing climate, combined with effects of UCEs as a result
212 of more frequent extreme drought/heat events and drought stress, can exacerbate and amplify
213 SOs and MOs (Jump et al., 2017), leading to increasing C loss, even though various buffering

214 mechanisms exist (cf. (Lloret et al., 2012; Allen et al., 2015)). Relative to our conceptual (Fig.
215 1d), we note that most experimental, observational and modeling studies (Ciais et al., 2005; da
216 Costa et al., 2010; Phillips et al., 2010; Meir et al., 2015) take into account only low to moderate
217 drought intensities (such as 50% rain excluded) or single events, or combine drought with
218 moderate effects of temperature change. Where there has been 100% rain exclusion, it was on
219 very small plots of 1.5 m² (Meir et al., 2015). As represented by the increasing amplitude of
220 oscillations in Fig. 1d, the interactions between increased temperatures, UCE events, and
221 vegetation feedbacks make ecosystem states become inherently unpredictable, particularly over
222 longer time-scales.

223

224 **2 Vegetation Demography Model (VDM) Approaches**

225 We argue that VDMs are well suited to address climate change impacts due to the
226 inclusion of detailed process representation of dynamic plant growth, recruitment, and mortality,
227 resulting in changes in abundance of different PFTs, as well as vertically stratified tree size- and
228 age-class structured ecosystem demography. Community dynamics and age-/size-structure are
229 emergent properties from competition for light, space, water, and nutrients, which dynamically
230 and explicitly scale up from the tree, to stand, to ecosystem level. Within this characterization,
231 VDMs also differ between each other and are set up in different configuration, allowing for
232 various testing capabilities. For full names of each model listed below and references, see Table
233 S1. For example, VDMs can aggregate and track the community level disturbance into either
234 patch-tiling sampling (e.g., ED2, FATES, LM3-PPA, ORCHIDEE, JSBACH4.0) or statistical
235 approximations (e.g., LPJ-GUESS, SEIB-DGVM, and CABLE-POP). VDMs could also vary in
236 representing light competition within either multiple canopy layers (e.g., ED2, FATES, LM3-
237 PPA, LPJ-GUESS, SEIB-DGVM) or in a single canopy (e.g., JSBACH4.0, ORCHIDEE,
238 CABLE-POP).

239 Powell et al. (2013) compared multiple VDMs and LSMs to interpret ecosystem
240 responses to long-term droughts in the Amazon and are informative when conducting model-data
241 comparisons, but studies of the cascade of ecosystem responses and mortality to UCEs are
242 lacking. In a cutting-edge area of development, new mechanistic implementation of plant
243 competition for water and plant hydraulics in VDMs (i.e., hydrodynamics) are improving our
244 understanding of plant-water relations and stresses within plants, such as with TFSv.1-Hydro

245 (Christoffersen et al., 2016), ED2-hydro (Xu et al., 2016), and FATES-HYDRO (Ma et al., 2021;
246 Fang et al., 2022). Compared to more simplistic representation of plant acquiring soil moisture
247 not connected to plant physiology (e.g., LPJ-GUESS, LM3-PPA, CABLE-POP, SEIB-DGVM).
248 For hydrodynamic representations in ‘big-leaf’ LSMs such as CLM5, JULES, and Noah-MP-
249 PHS see Kennedy et al., (2019), Eller et al., (2020), and Li et al., (2021) respectively.

250 The discussion section provides a deeper investigation of model response to UCEs related
251 to droughts. An exhaustive review of all VDMs, and all plant processes is too large to be done
252 here. Existing review papers of different VDM development, processes, and uncertainties can be
253 found here: Fisher et al., (2018); Bonan (2019); Trugman et al., (2019); Hanbury-Brown et al.
254 (2022); Bugmann and Seidl (2022); and specifically related to plant hydraulics see: Mencuccini
255 et al., (2019); Anderegg and Venturas (2020). We use LPJ-GUESS and ED2 as example VDMs
256 in an initial guide framework to explore hypotheses around vegetation mortality and integrated
257 carbon loss from UCEs and climate change impacts, and highlight limiting model processes.
258 Since field data needed to evaluate UCE responses are, by definition, unavailable, we do not
259 perform model-data comparisons. Rather, we use the model results and conceptual framework as
260 a road map to explore our hypotheses and illustrate their implications for ecosystem responses
261 under UCEs, not historical drought events.

262

263 **2.1 LPJ-GUESS and ED2 Model Descriptions**

264 We explored our hypotheses at forested ecosystems in Australia and Central America
265 using two VDMs: the Lund-Potsdam-Jena General Ecosystem Simulator (LPJ-GUESS) (Smith et
266 al., 2001; Smith et al., 2014) and the Ecosystem Demography model 2 (ED2) (Medvigy et al.,
267 2009; Medvigy and Moorcroft, 2012). Both LPJ-GUESS and ED2 resolve vegetation into tree
268 cohorts characterized by their PFT, in addition to age-class in LPJ-GUESS; and size, and stem
269 number density in ED2. Both models are driven by external environmental drivers (e.g.,
270 temperature, precipitation, solar radiation, atmospheric CO₂ concentration, nitrogen deposition),
271 and soil properties (soil texture, depth, etc.), and also depend on dynamic ecosystem state, which
272 includes light attenuation, soil moisture, and soil nutrient availability. Establishment and growth
273 of PFTs, and their carbon-, nitrogen- and water-cycles, are simulated across multiple patches per
274 grid cell to account for landscape heterogeneity. Both models characterize PFTs by physiological

275 and bioclimatic parameters, which vary between the models (Smith et al., 2001; Smith et al.,
276 2014; Medvigy et al., 2009; Medvigy and Moorcroft, 2012).

277 The LPJ-GUESS includes three woody PFTs: evergreen, intermediate evergreen, and
278 deciduous PFTs. Mortality in LPJ-GUESS is governed by a ‘growth-efficiency’-based function
279 ($\text{kg C m}^{-2} \text{ leaf yr}^{-1}$), which captures effects of water deficit, shading, heat stress, and tree size on
280 plant productivity relative to its resource-uptake capacity (leaf area), with a threshold below
281 which stress-related mortality risk increases markedly, in addition to background senescence and
282 exogenous disturbances. Stress mortality can be reduced by plants using labile carbon storage,
283 modeled implicitly using a ‘C debt’ approach, which buffers low productivity, enhancing
284 resilience to milder extremes (more details are given in section 4.1.4). Total mortality can thus be
285 impacted by variation in environmental conditions such as water limitation, low light conditions,
286 and nutrient constraints, as well as current stand structure (Smith et al., 2001; Hickler et al.,
287 2004).

288 The ED2 version used here (Xu et al., 2016) includes four woody PFTs: evergreen,
289 intermediate evergreen, deciduous, brevi-deciduous, and deciduous stem-succulent. This ED2
290 version includes coupled photosynthesis, plant hydraulics, and soil hydraulic modules (Xu et al.,
291 2016), which together determine plant water stress. The plant hydraulics module tracks water
292 flow along a soil–plant–atmosphere continuum, connecting leaf water potential, stem sap flow,
293 and transpiration, thus influencing controls on photosynthetic capacity, stomatal closure,
294 phenology, and mortality. Leaf water potential depends on time-varying environmental
295 conditions as well as time-invariant PFT traits. Leaf shedding is triggered when leaf water
296 potential falls below the turgor loss point (a PFT trait) for a sufficient amount of time. Leaf
297 flushing occurs when stem water potential remains high (above half of the turgor loss point) for a
298 sufficient time (see Xu et al., 2016 for details). PFTs differ in their hydraulic traits, wood
299 density, specific leaf area, allometries, rooting depth, and other traits. Stress-based mortality in
300 the ED2 version used here includes two main physiological pathways in our current
301 understanding of drought mortality (McDowell et al., 2013): C starvation and hydraulic failure.
302 Mortality due to C starvation in ED2 results from a reduction of C storage, a proxy for non-
303 structural carbohydrate (NSC) storage, which integrates the balance of photosynthetic gain and
304 maintenance cost under different levels of light and moisture availability. Mortality due to

305 hydraulic failure in ED2 is based on the percentage loss of stem conductivity. ED2 also includes
306 a density-independent senescence mortality rate based on wood density.

307 **2.2 Modeling guide**

308 To exemplify how VDMs can be tools to explore new hypotheses related to UCEs we
309 applied the models at two field sites, that were chosen due to being extensively studied and the
310 models used here have already been run at these sites and previously benchmarked against field
311 data (see Xu et al., 2016; Medlyn et al., 2016; Medvigy et al., 2019 for model-data validation).
312 The purpose of this paper was not to do a large multi-site comparison, but rather just select a few
313 for hypothesis testing. In addition, the two sites span a range of vegetation types and are in
314 warm, seasonally dry climates that are more likely to experience droughts in the future (Allen et
315 al., 2017). The first is a mature *Eucalyptus* (*E. tereticornis*) warm temperate-subtropical
316 transitional forest that is the site of the Eucalyptus Free Air CO₂ enrichment (EucFACE)
317 experiment in Western Sydney, Australia (Medlyn et al., 2016; Ellsworth et al., 2017; Jiang et
318 al., 2020). The second site is a seasonally dry tropical forest in the Parque Nacional Palo Verde
319 in Costa Rica (Powers et al., 2009). Site description details can be found in Supplement Text A.

320 We performed a 100-year “baseline” simulation for each model at each site driven by
321 constant, near ambient, atmospheric CO₂ (400 ppm) and recycled historical site-specific climate
322 data (1992-2011 for EucFACE and 1970-2012 for Palo Verde; Sheffield et al., (2006)), absent of
323 drought treatments. A detailed description of the meteorological data and initial conditions used
324 to drive the models is in the Supplementary Text A. The two models were previously tuned for
325 each site (Xu et al., 2016; Medlyn et al., 2016), and no additional site-level parameter tuning was
326 conducted here due to evaluating responses from hypothetical UCEs. To describe the ecosystem
327 impact of UCEs, we simulated 10 years of pre-drought conditions (continuing from the baseline
328 simulation), followed by drought treatments that differed in intensity and duration, followed by a
329 100-year post-drought recovery period. To explore the effects of drought intensity, we conducted
330 20 different artificial drought intensity simulations, in which precipitation during the whole year
331 is reduced by 5% to 100% of its original amount, in increments of 5%. To explore the effects of
332 drought duration, the 20 different drought intensities are maintained over 1, 2 and 4 years (Table
333 S2). We examined model responses of aboveground biomass, leaf area index (LAI), stem density
334 (number ha⁻¹), plant available soil water (mm), plant C storage (kg C m⁻²), change in stem
335 mortality rate (yr⁻¹), and PFT composition.

336 To explore how temperature, eCO₂ concentration, and UCE droughts influence forest C
 337 dynamics individually and in combination, we implemented the following five experimental
 338 scenarios, some realistic and others hypothetical, for each model (Table S2): increased
 339 temperature only (+2K over ambient), eCO₂ only (600 ppm and 800 ppm), and both increased
 340 temperature and eCO₂ (+2K 600 ppm; +2K 800 ppm). Temperature and eCO₂ manipulations
 341 were applied as step increases over the baseline conditions, and are artificial scenarios, as
 342 opposed to model-generated climate projections.

343

344 **2.3 Linking concepts, hypotheses, and model outcomes**

345 To relate our simulation results to Fig. 1a, we compared the total biomass loss as a result
 346 of each drought treatment by calculating the percentage of biomass reduction at the end of the
 347 drought period relative to the baseline (no drought) simulation. To explicitly consider biomass
 348 recovery rates over time, we calculated “integrated-C-loss” (Eqs. 1-3), as a result of drought
 349 under current climate, which are determined based on the concepts in Fig. 1b. We defined
 350 “integrated-C-loss” as the time-integrated carbon in biomass that is lost due to drought relative to
 351 what the vegetation would have stored in the absence of drought. That is, it is the difference
 352 between biomass in the presence of drought (B_d) at time (t) and biomass in the baseline
 353 simulation (no drought; B_{base}), integrated over a defined recovery time period (in kg C m⁻²
 354 yr):

$$\text{Integrated-C-loss} = \int_{t=t_1}^{t=t_2} (B_{base}(t) - B_d(t)) dt \quad (\text{Eq. 1})$$

355

356 To define the bounds of integration, in Eq. 1, t_1 is defined as the time when the maximum
 357 amount of plant C is lost as a result of the drought:

$$B_{base}(t_1) - B_d(t_1) = \max_t [B_{base}(t) - B_d(t)] \quad (\text{Eq. 2})$$

358

359 Then, t_2 is defined implicitly as the time when 50% of the lost biomass has been recovered
 360 compared to the baseline:

$$B_{base}(t_2) - B_d(t_2) = \frac{1}{2} (B_{base}(t_1) - B_d(t_1)) \quad (\text{Eq. 3})$$

361

362 Since all integrated-C-loss results are taken as the difference from a non-drought baseline
363 biomass (B_{base}) and all droughts will result in a loss of C.

364 We also use integrated-C-loss to examine the role of drought, temperature and eCO_2
365 change for moderating or exacerbating the impacts of drought on forest C stocks; i.e., to evaluate
366 the hypotheses illustrated in Fig. 1c. To assess these impacts of changing climates, we calculate
367 an “integrated-C-change” (Eq. 4). Defined as the difference between the integrated-C-loss due to
368 drought alone (Eqs. 1-3) under present climate, and the integrated-C-loss due to the combined
369 effects of drought and climate change (i.e., five scenarios of temperature increase and eCO_2):

$$\text{Integrated-C-change} = \text{integrated C Loss}_{\text{Drought}} - \text{integrated C Loss}_{\text{Drought+CC}} \quad (\text{Eq. 4})$$

370
371 Because we expect drought to reduce vegetation C stocks, and thus integrated-C-loss to
372 be negative, positive values of integrated-C-change indicate that changes in climatic drivers
373 reduced the C losses from drought (i.e., buffering effects). Negative values of integrated-C-
374 change indicate that the climate change scenario leads to either greater C losses or losses that
375 persist for longer amounts of time (i.e., magnitude and/or duration) compared to a simulation
376 with no climate change (i.e., “reference” run).

377

378 **3 Results**

379 As a basis for the treatment results presented here, we compared the baseline simulations
380 (prior to drought or climate change treatments) of the two VDMs to observations at both sites for
381 biomass and LAI (Table S3, Fig. S1). Both models had similar biomass compared to
382 observations at Palo Verde (10.4 - 11.7 vs. 11.0 $kgC\ m^{-2}$), and at EucFACE biomass matched
383 well in LPJ-GUESS (12.1 vs. 12.7 $kgC\ m^{-2}$) but was low in ED2 (5.6 $kgC\ m^{-2}$). Both models also
384 had similar LAI to observations at Palo Verde (3.3 – 4.5 vs. 3.8 (± 1.06) $m^2\ m^{-2}$), and at
385 EucFACE LAI matched well in ED2 (1.6 vs. 1.7 $m^2\ m^{-2}$), but was high for LPJ-GUESS (3.2 m^2
386 m^{-2}). At EucFACE LAI ranged from 1.2 to 2.1 over a 28-month measurement period (Duursma
387 et al., (2016), but LPJ-GUESS had very large fluctuations in annual LAI outside of these ranges
388 (Fig. S1). These models are well documented and investigated VDMs, with many studies that
389 have looked into parameter uncertainty (see Supplemental Text A for select references that
390 explore model/parameter sensitivity).

391 Both models displayed nonlinear responses to drought, in concurrence with Hypothesis
392 H1, but they differ in their behavior and between sites. In general, ED2 shows sensitivity to
393 drought duration (Hypothesis H1b), while LPJ-GUESS shows a stronger sensitivity to drought
394 intensity (Hypothesis H1a). ED2's sensitivity to the duration of drought was mild at Palo Verde
395 (Fig. 2a), and stronger at EucFACE particularly during the 4-year drought with a strong non-
396 monotonic pattern (see explanation below) (Fig. 2b). When reporting only percentage of biomass
397 loss, ED2 predicts close to no UCE response at Palo Verde; with a maximum biomass reduction
398 of only 40% during 95% precipitation removal and a 4-year drought event (i.e., UCE). LPJ-
399 GUESS shows very little sensitivity to drought duration but is highly sensitive to drought
400 intensity. C loss predicted by LPJ-GUESS at Palo Verde reached a threshold at ~65% drought
401 intensity, after which forests exhibit strong biomass losses, up to 100% (Fig. 2a). At the
402 EucFACE site, both models predict a critical threshold of biomass loss at 35%-45% drought
403 intensity, with LPJ-GUESS predicting total biomass loss (up to 100%) after this drought
404 intensity threshold (Fig. 2b). The EucFACE drought threshold is lower than that of the
405 seasonally dry mixed tropical forest in Palo Verde.

406 With respect to C loss over a recovering time period (integrated-C-loss), the two models
407 predict similar drought responses at Palo Verde (Fig. 2c), but not at EucFACE (Fig. 2d). At Palo
408 Verde, the similarity between models in integrated-C-loss reflected longer biomass recovery time
409 but less biomass loss in the short-term in ED2 relative to LPJ-GUESS, which predicted greater
410 biomass loss immediately after drought but shorter recovery time. With the exception of the 1-
411 year drought in ED2, both models predict similar integrated-C-loss across a range of UCEs at
412 Palo Verde, via different pathways. The integrated-C-loss metric revealed a strong nonlinear
413 response to drought duration in ED2 (Fig. 2c), while this nonlinearity is less evident when only
414 examining change in biomass (Fig. 2a). The "V"-shaped patterns observed particularly in Fig.
415 2b, arise from interactions between whole-leaf phenology and stomatal responses to drought in
416 ED2. For drought intensities lower than 40%, stomatal conductance is reduced but leaves are not
417 fully shed. Leaf respiration continues, gradually depleting non-structural C pools, followed by a
418 loss of biomass. However, for higher drought intensities, leaf water potentials quickly become
419 systematically lower than leaf turgor loss points and tree cohorts shed all their leaves. This
420 strategy represents an immediate loss of C via leaf shedding, but spares the cohort from slow,
421 respiration-driven depletion of C stocks.

422

423 **3.1 Predicted model responses to UCE droughts combined with increased temperature** 424 **and/or eCO₂**

425 Relating to our second hypothesis of additional effects of warming and eCO₂, we tested
426 15 treatments in total, repeating the five climate change scenarios for each of the three drought
427 durations. With the addition of climate change impacts, ED2 remained sensitive to the duration
428 of drought, with warming negatively impacting integrated-C-change and most consistently
429 during 2- and 4-year drought durations. ED2 predicts that during the 2- and 4-year droughts at
430 EucFACE, losses are exacerbated when accompanied with warming, even with eCO₂, with 600
431 ppm having a more detrimental impact than the more elevated 800 ppm (Fig. 3b-c). The average
432 integrated-C-change was -111.0 kg C m⁻² yr across all 15 treatments (Table 2). Only during the
433 1-year drought duration did drought plus warming and eCO₂ have a buffering effect on C stocks,
434 seen in four out of our five scenarios but only during relatively modest droughts intensities (Fig.
435 3a; i.e., positive integrated-C-change, see also Table 2).

436 The ED2 simulations of the seasonally dry Palo Verde site (Fig. 3d-f), produced less
437 frequent negative impacts on drought and climate change driven C losses compared to
438 EucFACE, with an average integrated-C-change of -53.9 kg C m⁻² yr⁻¹ across all 15 treatments
439 (Table 2). During the 2-year drought, applying +2K with eCO₂ to 600 ppm showed a slight
440 buffering effect to droughts and the most consistent positive integrated-C-change (Fig. 3e; Table
441 2). Interestingly, an increase in only eCO₂ to 800 ppm (no warming) when applied with the 2-
442 and 4-year droughts resulted in the largest loss in integrated-C-change (Fig. 3e-f), larger than the
443 expected 'most severe' scenario; +2K and 800 ppm.

444 Similar to ED2, the LPJ-GUESS model showed a nearly complete negative response in
445 integrated-C-change as a result of UCE drought and scenarios of warming and eCO₂ at the
446 EucFACE site (Fig. 3g-i), but mixed and more muted results at Palo Verde (Fig. 3j-l, Table 2).
447 The average integrated-C-change relative to the reference case was -95.4 at EucFACE and -7.8
448 kg C m⁻² yr at Palo Verde, both less negative compared to ED2. One notable pattern was up until
449 a drought intensity threshold of ~40%, the climate scenarios had no effect or response in
450 integrated-C-change at EucFACE, and the muted response from warming and eCO₂ Palo Verde,
451 compared to ED2. Surprisingly, the +2K scenario switched the integrated-C-change to positive,
452 compared to the reference case (Fig. 3g-i; red lines), potentially a physiological process in the

453 model to increased temperatures only that signals an anomalous resiliency response. Similar to
454 the results with no climate change, LPJ-GUESS remained sensitive to the intensity of drought,
455 with ~40% precipitation reduction being a threshold.

456 The models and sites differed with regard to SO and MO responses to increasing drought
457 severity and its interactions with warming and eCO₂ (related to conceptual Fig. 1d). ED2 showed
458 a more consistent MO response during UCEs and with additional warming and eCO₂ (Fig. 3;
459 negative integrated-C-change), especially at EucFACE, suggesting these ecosystems will remain
460 in a depressed carbon condition driving vegetation mortality, and/or longer recoveries. LPJ-
461 GUESS produced more opportunities for SO with climate change. For example, at EucFACE
462 CO₂ fertilization created small SO periods that then led to MO with increasing drought severities,
463 and at Palo Verde all +2K and 600 ppm led to a SO (Fig. 3j-l; Table 2).

464 Both models predicted that C losses due to drought interactions with increased
465 temperature and eCO₂ were less severe at the seasonally dry Palo Verde site compared to the
466 somewhat less seasonal, more humid EucFACE site (Table 2), which could be attributed to
467 higher diversity in PFT physiology at Palo Verde. Palo Verde's community composition that
468 emerged following drought included either three (LPJ-GUESS) or four (ED2) PFTs, while only a
469 single PFT existed at EucFACE. With rising temperatures under climate change, UCEs will be
470 hotter and drier. Nine out of the twelve simulations with both +2K and 600 ppm CO₂, and all but
471 one +2K and 800 ppm CO₂ produced a negative integrated-C-change, implying stronger C losses
472 and/or longer recovery times when droughts are exacerbated by increasing temperatures (Table
473 2).

474

475 **4 Discussion**

476 Vegetation demographic models (VDMs) allowed us to uniquely explore two hypotheses
477 regarding a range of modeled response of terrestrial ecosystems to unprecedented climate
478 extremes (UCEs), and setting the stage for the following perspectives to help guide future
479 research. Key model results include strong nonlinearities (Hypothesis H1) in C response to
480 extreme drought *intensities* in LPJ-GUESS and alternatively drought *durations* in ED2 (at one of
481 two sites), with differences in thresholds between the two models and ecosystems. These
482 nonlinearities may arise from multiple mechanisms that we begin to investigate here, including
483 shifts in plant hydraulics or other functional traits, C allocation, phenology, stand size-structure

484 and/or age demography, and compositional changes, all which vary among ecosystem types. A
485 critical look of driving model mechanisms, which emerged from the hypothetical drought
486 simulations used here, are summarized in Table 3. The models also show exacerbated biomass
487 loss and recovery times in the majority of our scenarios of warming and eCO₂, supporting
488 Hypothesis H2. Below, we discuss the underlying mechanisms that drive simulated ecosystem
489 response to UCEs using the models and sites as conceptual “experimental tools” and
490 observational evidence from the literature. We focus on two temporal stages of the UCE: The
491 pre-drought ecosystem stage characterized as the quasi-stable state of the ecosystem prior to a
492 UCE, which can mediate ecosystem resistance and disturbance impact, and the post-drought
493 recovery stage (Table 1).

494

495 **4.1 The role of ecosystem processes and states prior to UCEs**

496 **4.1.1 The role of phenology and phenological strategies prior to UCEs:**

497 Observations show that diversity of deciduousness contributes to successful alternative
498 strategies for tropical forest response to water stress (Williams et al., 2008). For example, during
499 the severe 1997 El Nino drought, brevi-deciduous trees and deciduous stem-succulents within a
500 tropical dry site in Guanacaste Costa Rica retained leaves during the extreme wet-season
501 drought, behaving differently than during normal dry seasons (Borchert et al., 2002). Both
502 models here predict that neither seasonal deciduousness, nor drought-deciduous phenology at the
503 seasonally dry tropical forest, Palo Verde (which consists of trees with different leaf
504 phenological strategies), act to buffer the forest from a large drop in LAI during UCEs (Fig. S1a-
505 b). Even with this large decrease in LAI, ED2 predicted a very weak biomass loss at the time of
506 UCEs (Fig. 2a), suggesting large-scale leaf loss is not a direct mechanism of plant mortality in
507 ED2. Leaf loss is one component of total carbon turnover flux equations in terrestrial models, in
508 addition to woody loss, fine-roots, and reproductive tissues. Having a better understanding of
509 when extreme levels of phenological turnover contribute to stand-level mortality could be
510 improved. Among other turnover hypothesis explored, Pugh et al. (2020) found that phenological
511 turnover fluxes were just as important as mortality fluxes in driving forest turnover time in the
512 VDMs: LPJ-GUESS, CABLE-POP, ORCHIDEE, but not the LSM JULES. At the EucFACE
513 site prior to the simulated extreme drought, LPJ-GUESS displayed strong inter-annual variability

514 in LAI (Fig. S1a-b). This capability of large swings in LAI (5.8 to 0.8) by LPJ-GUESS could
515 contribute to model uncertainty and the considerable mortality response at EucFACE. Modeled
516 LAI was the largest source of variability in another ecosystem model, CABLE, when evaluating
517 the simulated response to CO₂ fertilization (Li et al., 2018). VDMs could be improved by better
518 capturing different plant phenological responses to UCEs by better representing a range of leaf-
519 level morphological and physiological characteristics relevant to plant-water relations such as
520 leaf age, retention of young leaves even during extreme droughts, (Borchert et al., (2002)), and
521 variation in hydraulic traits as a function of leaf habit (Vargas et al., (2021)) (Table 3). Two such
522 examples are seen in the FATES model where the possibility for “trimming” the lowest leaf
523 layer can occur when leaves are in negative carbon balance due to light limitation thus
524 optimizing maintenance costs and carbon gain, as well as leaf age classifications providing
525 variations in leaf productivity and turnover.

526

527 **4.1.2 The role of plant hydraulics prior to UCEs:**

528 Susceptibility of plants to hydraulic stress is one of the strongest determinants of
529 vulnerability to drought, with loss of hydraulic conductivity being a major predictor of drought
530 mortality in temperate (McDowell et al., 2013; Anderegg et al., 2015; Sperry and Love, 2015;
531 Venturas et al., 2021) and tropical forests (Rowland et al., 2015; Adams et al., 2017b), as well as
532 a tractable mortality mechanism to represent in process-based models (Choat et al., 2018,
533 Kennedy et al., 2019). Both LPJ-GUESS and ED2 exhibited a wide range in amount and pattern
534 of plant-available-water prior to drought (Fig. S1c-d), contributing to large differences in UCE
535 response. LPJ-GUESS, which does not simulate hydrodynamics, predicted lower total plant-
536 available-water at both sites compared to ED2, and subsequently simulated greater mortality and
537 a greater increase in plant-available-water right after the UCEs as a result of less water demand.
538 Due to ED2 using a static mortality threshold from conductivity loss (88%), it likely does not
539 accurately reproduce the wide range of observations of drought-induced mortality. In ED2, large
540 trees, with longer distances to transport water, were at higher risk and suffered higher mortality
541 (Fig. 4), demonstrating how stand demography, size structure, and tapering of xylem conduits
542 can play an important role in ecosystem models (Petit et al., 2008; Fisher et al., 2018). Of the
543 VDMs that are beginning to incorporate a continuum of hydrodynamics (e.g., ED2 (described in
544 Methods 2.1 section) and FATES-HYDRO (Fang et al., 2022, based on Christoffersen et al.,

2016), they are able to solve for transient water from soils to roots, through the plant and connect with transpiration demands. Therefore instead of the plant water stress function being based on soil water potentials, it is replaced with more realistic connections with leaf water potentials. Mortality is then caused by hydraulic failure via embolism controlled by the critical water potential (P_{50}) that leads to 50% loss of hydraulic conductivity. For advancements in tree level hydrodynamic modeling see the FETCH3 model (Silva et al., 2022), for justification for plant hydrodynamics in conjunction with multi-layer vertical canopy profiles see Bonan et al., (2021). There are strong interdependencies and related mechanisms connecting both hydraulic failure (e.g., low soil moisture availability) and C limitation (e.g., stomatal closure) during drought (McDowell et al., 2008; Adams et al., 2017b), and these interactions should be incorporated in ecosystem modeling and further explored (Table 3).

4.1.3. The role of carbon allocation prior to UCEs:

Plants have a variety of strategies to buffer vulnerability to water and nutrient stress caused by extreme droughts, such as allocating more C to deep roots (Joslin et al., 2000; Schenk and Jackson, 2005), investing in mycorrhizal fungi (Rapparini and Peñuelas, 2014), or reducing leaf area without shifting leaf nutrient content (Pilon et al., 1996). Alternatively, presence of deep roots doesn't necessarily lead to deep soil moisture utilization, as seen in a 6-year Amazonian throughfall exclusion experiment where deep root water uptake was still limited, even with high volumetric water content (Markewitz et al., 2010). Elevated CO_2 alone will enhance growth and water-use efficiency (Keenan et al., 2013), reducing susceptibility to drought. However, such increased productivity within a forest stand, and associated structural overshoot during favorable climate windows, can also be reversed by increased competition for light, nutrients, and water during unfavorable UCEs – potentially leading to mortality overshoot (Fig. 1d) and higher C loss. Mortality overshoot, as a result of structural overshoot, could be an explanation for the negative integrated-C-change (i.e., C loss) in the majority of eCO_2 -only simulations (18 out of 24 scenarios; Table 2).

Effects of CO_2 fertilization on plant C allocation strategies are uncertain. As a result, ecosystem models differ in their assumptions on controls of C allocation in response to eCO_2 , leading to divergent plant C use efficiencies (Fleischer et al., 2019). Global scale terrestrial models are beginning to include optimal dynamic C allocation schemes, over fixed ratios, that account for concurrent environmental constraints on plants, such as water, and adjust allocation

576 based on resource availability such as in LM3-PPA (Weng et al., 2015), but the representation of
577 C allocation is still debated and progressing (De Kauwe et al., 2014; Montané et al., 2017; Reyes
578 et al., 2017). Options for carbon allocation strategies can be based on the allometric partitioning
579 theory (i.e., allocation follows a power allometry function between plant size and organs which
580 is insensitive to environmental conditions; Niklas, 1993), as an alternative to ratio-based optimal
581 partitioning theory (i.e., allocation to plant organs based on the most limiting resources)
582 (McCarthy and Enquist, 2007) or fixed ratios (Table 3), and the strategies should be further
583 investigated particularly due to VDMs substantial use of allometric relationships. A meta-
584 analysis of 164 studies found that allometric partitioning theory outperformed optimal
585 partitioning theory in explaining drought-induced changes in C allocation (Eziz et al., 2017).
586 Further eco-evolutionarily-based approaches such as optimal response or game-theoretic
587 optimization, as well as entropy-based approaches are useful when wanting to simulate higher
588 levels of complexity (reviewed in Franklin et al. 2012). With more frequent UCEs and the need
589 for plants to reduce water consumption, a shift in the optimal strategy of allocation between
590 leaves and fine roots should change. The goal functions (e.g., fitness proxy) used in optimal
591 response modeling can account for these shifts in costs and benefits of allocation between all
592 organs (Franklin et al. 2009, 2012).

593

594 **4.1.4 The role of plant carbon storage prior to UCEs:**

595 Studies of neotropical and temperate seedlings show that pre-drought storage of non-
596 structural carbohydrates (NSCs) provides the resources needed for growth, respiration
597 osmoregulation, and phloem transport when stomata close during subsequent periods of water
598 stress (Myers and Kitajima, 2007; Dietze and Matthes, 2014; O'Brien et al., 2014). Furthermore,
599 direct correlations have been shown between NSC depletion and embolism accumulation, and
600 the degree of pre-stress reserves and utilization of soluble sugars (Tomasella et al., 2020). The
601 amount of NSC storage required to mitigate plant mortality during C starvation and interactions
602 with hydraulic failure from severe drought is difficult to quantify, due to the many roles of NSCs
603 in plant function and metabolism (Dietze and Matthes, 2014). For example, NSCs were not
604 depleted after 13 years of experimental drought in the Brazilian Amazon (Rowland et al., 2015).
605 As atmospheric CO₂ increases with climate change, NSC concentrations may increase, as seen in
606 manipulation experiments (Coley, 2002), but interactions with heat, water stress, enhanced leaf

607 shedding, and nutrient limitation complicates this relationship, and needs to be further explored.
608 Despite the recognition of the critical role that plant hydraulic functioning and NSCs play in tree
609 resilience to extremes, knowledge gaps and uncertainties preclude fully incorporating these
610 processes into ecosystem models.

611 Compared to ED2, LPJ-GUESS predicted low plant carbon storage (a model proxy for
612 NSCs) prior to and during drought, and at times became negative, thereby creating C costs (Fig.
613 S2a-b), leading to C starvation and potentially explaining the larger biomass loss in LPJ-GUESS
614 at both sites. Alternatively, ED2 maintained higher levels of NSCs providing a buffer to stress,
615 and mitigating the negative effects of drought. Maintenance of NSCs in ED2, even during
616 prolonged drought (at EucFACE) is due to: (1) trees resorbing a fraction of leaf C during leaf
617 shedding, (2) no maintenance costs for NSC storage in the current version, and (3) no allocation
618 of NSCs to structural growth until NSC storage surpasses a threshold (the amount of C needed to
619 build a full canopy of leaves and associated fine roots), allowing for a buffer to accumulate. In
620 LPJ-GUESS, accumulation and depletion of NSC is recorded as a ‘C debt’ being paid back in
621 later years. The contrasting responses of the two models to drought, and the likely role of NSCs
622 in explaining differences in model behavior, highlights the need to better understand NSC
623 dynamics and to accurately represent the relevant processes in models (Richardson et al., 2013;
624 Dietze and Matthes, 2014). More observations of C accumulation patterns and how/where NSCs
625 drive growth, respiration, transport and cellular water relations would enable a more realistic
626 implementation of NSC dynamics in models (Table 3).

627

628 **4.1.5 Role of functional trait diversity prior to UCEs:**

629 Currently LPJ-GUESS simulates the Palo Verde community using three PFTs, while ED2 uses
630 four PFTs that differ in photosynthetic and hydraulic traits. The community composition simulated by
631 ED2 is shown to be more resistant to UCEs compared to LPJ-GUESS (Fig. 5), perhaps due to
632 relatively higher functional diversity (via more PFTs with additional phenological and hydraulic
633 diversity). This additional diversity helps to buffer ecosystem response to drought by allowing more
634 tolerant PFTs to benefit from reductions in less-tolerant PFTs, thus buffering reductions in ecosystem
635 function (Anderegg et al., 2018). Higher diversity ecosystems were found to protect individual species
636 from negative effects of drought (Aguirre et al., 2021) and enhance productivity resilience following

637 wildfire (Spasojevic et al., 2016); thus, functionally diverse communities may be key to enhancing
638 tolerance to rising environmental stress.

639 Recent efforts to consolidate information on plant traits (Reich et al., 2007; Kattge et al., 2011)
640 have contributed to identifying relationships that can impact community-level drought responses
641 (Skelton et al., 2015; Anderegg et al., 2016a; Uriarte et al., 2016; Greenwood et al., 2017), such as
642 life-history characteristics, and strategies of resource acquisition and conservation as predictors of
643 ecosystem resistance (MacGillivray et al., 1995; Ruppert et al., 2015). While adding plant trait
644 complexity in ESMs may be required to accurately simulate key vegetation dynamics, it necessitates
645 more detailed parameterizations of processes that are not explicitly resolved (Luo et al., 2012). Further
646 investigation of how VDMs represent interactions leading to functional diversity shifts is crucial to
647 this issue. Enquist and Enquist, (2011), as an example, show that long-term patterns of drought (20-
648 years) have led to increases in drought-tolerant dry forest species, which could modulate resistance to
649 future droughts. Higher diversity of plant physiological traits and drought-resistance strategies is
650 expected to enhance community resistance to drought, and models should account for shifts in diverse
651 functionality (Table 3).

652

653 **4.2 The role of ecosystem processes and states in post-UCE recovery**

654 **4.2.1 The role of soil water resources post-UCes:**

655 Our simulation results generally demonstrated a fast recovery of plant-available-water
656 and LAI at both sites (Fig. S1). Annual plant-available-water substantially increased right after
657 drought by an average of 163 mm at Palo Verde and 213 mm at EucFACE in the LPJ-GUESS
658 simulations, compared to much lower increases in ED2 (50 mm and 12 mm at Palo Verde and
659 EucFACE). This increase in available water post-drought can be attributed to reduced stand
660 density and water competition (Fig. S2c-d; diamonds vs. circles), alleviating the demand for soil
661 resources (water) and subsequent stress, which has also been shown in observations (McDowell
662 et al., 2006; D'Amato et al., 2013). After large canopy tree mortality events there can be
663 relatively rapid recovery of forest biogeochemical and hydrological fluxes (Biederman et al.,
664 2015; Anderegg et al., 2016b; Biederman et al., 2016). These crucial fluxes strongly influence
665 plant regeneration and regrowth, which can buffer ecosystem vulnerability to future extreme
666 droughts. However, this enhanced productivity has a limit. In a scenario where UCes continue to

667 intensify, causing greater reductions in soil water and reduced ecosystem recovery potential, the
668 SO growth that typically occurs after UCEs may be dampened (Fig. 1d). In water-limited
669 locations, similar to the dry forest sites used here, initial forest recovery from droughts were
670 faster due to thinning induced competitive-release of the surviving trees, and shallow roots not
671 having to compete with neighboring trees for water, allowing for more effective water user
672 (Tague and Moritz, 2019), stressing the importance of root competition and distribution in
673 models (Goulden and Bales, 2019). Tague and Moritz, (2019) also reported that this increased
674 water use efficiency and SO ultimately lead to water stress and related declines in productivity,
675 similar to the MO concept (Jump et al., 2017; McDowell et al., 2006). Since a core strength of
676 VDMs is predicting stand demography during recovery, improved quantification of density-
677 dependent competition following stand dieback would be beneficial for model benchmarking
678 (Table 3).

679

680 **4.2.2 The role of lagged turnover and secondary stressors post-UCEs:**

681 Time lags in forest compositional response and survival to drought could indicate
682 community resistance or shifts to more competitive species and competitive exclusion. During a
683 15-year recovery period from extreme drought at Palo Verde, LPJ-GUESS predicted an increase
684 in stem density (stems $\text{m}^2 \text{yr}^{-1}$) (Fig. S2c) compared to ED2, which predicted almost no impact in
685 stem recovery. The mortality “spike” in ED2 due to drought was muted and slightly delayed,
686 contributing to ED2’s lower biomass loss and more stable behavior of plant processes over time
687 at Palo Verde. At EucFACE, both models exhibited a pronounced lag effect in stem turnover
688 response, i.e. ~8-12 years after drought (Fig. S2d). After about a decade, strong recoveries and
689 increased stem density occurred, which in ED2 was followed by delayed mortality/thinning of
690 stems. Delayed tree mortality after droughts is common due to optimizing carbon allocation and
691 growth (Trugman et al., 2018), but typically only up to several years post-drought, not a decade
692 or more as seen in the model.

693 The versions of the VDMs used here do not directly consider post-drought secondary
694 stressors such as infestation by insects or pathogens, and the subsequent repair costs due to stress
695 damage, which could substantially slow the recovery of surviving trees. Forest ecologists have
696 long recognized the susceptibility of trees under stress, particularly drought, to insect attacks and

697 pathogens (Anderegg et al., 2015). Tight connections between drought conditions and increased
698 mountain pine beetle activity have been observed (Chapman et al., 2012; Creeden et al., 2014),
699 and can ultimately lead to increased tree mortality (Hubbard et al., 2013). Leaf defoliation is a
700 major concern from insect outbreaks following droughts, and can have large impacts on C
701 cycling, plant productivity, and C sequestration (Amiro et al., 2010; Clark et al., 2010; Medvigy
702 et al., 2012). Implementing these secondary stressors in models could slow the rate of post-UCE
703 recovery and lead to increased post-UCEs tree mortality.

704

705 **4.2.3 The role of stand demography post-UCEs:**

706 Change in stand structure is an important model process to capture, because large trees
707 have important effects on C storage, community resource competition, and hydrology
708 (Wullschleger et al., 2001) (Table 3), and maintaining a positive carbohydrate balance is
709 beneficial in sustaining (or repairing) hydraulic viability (McDowell et al., 2011). There is
710 increasing evidence, both theoretical (McDowell and Allen, 2015) and empirical (Bennett et al.,
711 2015; Rowland et al., 2015; Stovall et al., 2019), that large trees (particularly tall trees with high
712 leaf area) contribute to the dominant fraction of dead biomass after drought events. Under rising
713 temperatures (and decreasing precipitation), VPD will increase, leading to a higher likelihood of
714 large tree death (Eamus et al., 2013; Stovall et al., 2019), driving MO events as hypothesized in
715 Fig. 1d. Consistent with this expectation, ED2 predicted that the largest trees (>100 cm)
716 experienced the largest decreases in basal area to compared to all other size classes (Fig. 4). This
717 drought-induced partial dieback and mortality of large dominant trees has substantial impacts on
718 community-level C dynamics, as long-term sequestered C is liberated during the decay of new
719 dead wood (Palace et al., 2008; Potter et al., 2011). In ED2, the intermediate size class (60 - 80
720 cm) increased in basal area following large-tree death, taking advantage of the newly open
721 canopy space. However, small size classes do not necessarily benefit from canopy dieback. For
722 example, in a dry tropical forest, prolonged drought led to a decrease in understory species and
723 small-sized stems (Enquist and Enquist, 2011).

724 Due to VDMs being able to exhibit dynamic biogeography they are more useful at
725 predicting shifts in community composition beyond LSMs capabilities. Further areas of
726 advancement (described in Franklin et al. (2020)) is including models of natural selection, self-
727 organization, and entropy maximization which can substantially improve community dynamic

728 responses in varying environments such as UCEs. Eco-evolutionary optimality (EEO) theory can
729 also help improve functional trait representation in global process-based models (reviewed in
730 Harrison et al., 2021), through hypotheses in plant trait trade-offs and mechanistic links between
731 processes such as resource demand, acquisition, and plant's competitiveness and survival; traits
732 associated with high degrees of sensitivity in models. The power of prognostic VDMs to predict
733 shifts in demography and community migration with climate change is large, but rarely is being
734 constrained with plant-level EEO theory, and thus will likely need to use stand level competition
735 and coexistence principles of how plants self-organize (Franklin et al. 2020).

736

737 **4.2.4 The role of functional trait diversity & plant hydraulics post-UCEs:**

738 In field experiments, higher disturbance rates have shifted the recovery trajectory and
739 competition of the plant community towards one that is composed of opportunistic, fast-growing
740 pioneer tree species, grasses (Shiels et al., 2010; Carreño-Rocabado et al., 2012), and/or
741 deciduous species, as also seen in model results (Hickler et al., 2004). In the treatments presented
742 here, deciduous PFT types were also the strongest to recover after 15 years in both models,
743 surpassing pre-drought values (Fig. 5). It should be noted that ED2 exhibited a strong recovery in
744 the evergreen PFT as well, inconsistent with the above literature (Fig. 5b). PFTs in ED2 respond
745 to drought conditions via stomatal closure and leaf shedding, buffering stem water potentials
746 from falling below a set mortality threshold (i.e., 88% of loss in conductivity). This conductivity
747 threshold may need to be reconsidered if further examination reveals an unrealistic advantage
748 under drought conditions for evergreen trees, which exhibited a lower impact from droughts
749 (compared to deciduous and brevi-deciduous PFTs) in ED2. Nitrogen cycling feedbacks were
750 not investigated here, but could also be an explanation for a strong evergreen PFT recovery.

751 Recovery of surviving trees could be hindered by the high cost of replacing damaged
752 xylem associated with cavitation (McDowell et al., 2008; Brodribb et al., 2010). Many studies
753 have identified “drought legacy” effects of delayed growth or gross primary productivity
754 following drought (Anderegg et al., 2015; Schwalm et al., 2017) and the magnitude of these
755 legacies across species correlates with the hydraulic risks taken during drought itself (Anderegg
756 et al., 2015). The conditions under which xylem can be refilled remain controversial, but it seems
757 likely that many species, particularly gymnosperms, may need to entirely replace damaged

758 xylem (Sperry et al., 2002), and trees worldwide operate within narrow hydraulic safety margins,
759 suggesting that trees in all biomes are vulnerable to drought (Choat et al., 2012). The amount of
760 damaged xylem from a given drought event and recovery rates also vary across trees of different
761 sizes (Anderegg et al., 2018).

762 Plasticity in nutrient acquisition traits, intraspecific variation in plant hydraulic traits
763 (Anderegg et al., 2015), and changes in allometry (e.g., Huber values) can have large effects on
764 acclimation to extreme droughts. This suggests some capacity for physiological adaptation to
765 extreme drought, as seen by short-term negative effects from drought and heat extremes being
766 compensated for in the longer term (Dreesen et al., 2014). Still, given the shift towards more
767 extreme droughts with climate change, vegetation mortality thresholds are likely to be exceeded,
768 as reported in Amazonian long-term plots where mortality of wet-affiliated genera has increased
769 while simultaneously new recruits of dry-affiliated genera are also increasing (Esquivel-Muelbert
770 et al., 2019). Increasing occurrences of heat events, water stress and high VPD will lead to
771 extended closure of stomata to avoid cavitation, progressively reducing CO₂ enrichment benefits
772 (Allen et al., 2015). Where CO₂ fertilization has been seen to partially offset the risk of
773 increasing temperatures, the risk response was mediated by plant hydraulic traits (Liu et al.,
774 2017) using a soil–plant–atmosphere continuum (SPAC) model, yet interactions with novel
775 extreme droughts were not considered. The VDM simulations suggest that the combination of
776 elevated warming and potential structural overshoot from eCO₂ (or inaccurate representation in
777 NSCs allocation/usage priority) will exacerbate consequences of UCEs by reductions in both C
778 stocks and post-drought biomass recovery speeds (Fig. 3). Therefore, future UCE recovery may
779 not be easily predicted from observations of historical post-disturbance recovery. An associated
780 area for further investigation is to better understand the hypothesized interplay between
781 amplified mortality from hotter UCEs followed by structural overshoot regrowth during wetter
782 periods (Fig. 1d), which could potentially lead to continual large swings in MO and SO and
783 vulnerable net ecosystem C fluxes through time (Table 3).

784

785 **5 Summary of perspectives for model advancement**

786 Model limitations and unknowns exposed by our simulations and literature review
787 highlight current challenges in our ability to understand and forecast UCE effects on ecosystems.
788 These limitations reflect a general lack of empirical experiments focused on UCEs. Insufficient

789 data means that relevant processes may currently be poorly represented in models, and models
790 may then misrepresent C losses during UCEs. The two VDMs used here had different
791 sensitivities to drought duration and intensity. These model uncertainties could potentially be
792 addressed by improved datasets on thresholds of conductivity loss at high drought intensities, the
793 role of trait diversity (e.g., different strategies of drought deciduousness and EEO theory) in
794 buffering ecosystem drought responses, and a better grasp of allocation to plant C storage stocks
795 before, during, and after multi-year droughts. Our study takes some initial steps to identify and
796 assess model gaps in terms of mechanisms and magnitudes of responses to UCEs, which can
797 then be used to inform and develop field experiments targeting key knowledge gaps as well as to
798 prioritize ongoing model development (Table 3). Our intention was not to do an exhaustive list
799 of UCE simulation experiments, and additional modeling perturbations and experiments would
800 be useful outcomes of future studies. For example, we begin to investigate duration of droughts
801 but we did not consider frequency of back-to-back UCEs. This iterative model-experiment
802 framework of using VDMs as hypothesis testing tools offers strong potential to drive progress in
803 improving our understanding of terrestrial ecosystem responses to UCEs and climate feedbacks,
804 while informing the development of the next generation of models.

805 *Code Availability.* The source code for the ED2 model can be downloaded and available publicly
806 at <https://github.com/EDmodel/ED2>. The source code for the LPJ-GUESS model can be
807 downloaded and available publicly at <http://web.nateko.lu.se/lpj-guess/download.html>. All model
808 simulation data will be available in a Dryad repository.
809

810 *Data Availability.* Authors received the required permissions to use the site level meteorological
811 data used in this study. Otherwise, no ecological or biological data were used in this study.
812

813 *Author Contributions.* JH wrote the manuscript with significant contributions from AR, BS, JD,
814 DM, with input and contributions from all authors. XX and MM were the primary leads running
815 the model simulations, with model assistance and strong feedback from DM and BS. All authors
816 made contributions to this article, and agree to submission.
817

818 *Competing Interests.* The contact author has declared that neither they nor their co-authors have
819 any competing interests.
820

821 *Special Issue Statement.* Special Issue titled “Ecosystem experiments as a window to future
822 carbon, water, and nutrient cycling in terrestrial ecosystems”
823

824 *Financial Support:* Funding for the meetings that facilitated this work was provided by NSF-
825 DEB-0955771: An Integrated Network for Terrestrial Ecosystem Research on Feedbacks to the
826 Atmosphere and ClimatE (INTERFACE): Linking experimentalists, ecosystem modelers, and
827 Earth System modelers, hosted by Purdue University; as well as Climate Change Manipulation
828 Experiments in Terrestrial Ecosystems: Networking and Outreach (COST action ClimMani –
829 ES1308), led by the University of Copenhagen. J.A. Holm’s time was supported as part of the
830 Next Generation Ecosystem Experiments-Tropics, funded by the U.S. Department of Energy,
831 Office of Science, Office of Biological and Environmental Research under Contract DE-AC02-
832 05CH11231. AR acknowledges funding from CLIMAX Project funded by Belmont Forum and
833 the German Federal Ministry of Education and Research (BMBF). BS and MM acknowledge
834 support from the Strategic Research Area MERGE. W.R.L.A. acknowledges funding from the
835 University of Utah Global Change and Sustainability Center, NSF Grant 1714972, and the
836 USDA National Institute of Food and Agriculture, Agricultural and Food Research Initiative
837 Competitive Programme, Ecosystem Services and Agro-ecosystem Management, grant no. 2018-
838 67019-27850. JL acknowledges support from the Northern Research Station of the USDA Forest
839 Service (agreement 16-JV-11242306-050) and a sabbatical fellowship from sDiv, the Synthesis
840 Centre of iDiv (DFG FZT 118, 202548816). CDA acknowledges support from the USGS Land
841 Change Science R&D Program.
842

843 *Acknowledgements.* We thank Belinda Medlyn and David Ellsworth of the Hawkesbury Institute
844 for the Environment, Western Sydney University, for providing the meteorological forcing data
845 series for the EucFACE site, a facility supported by the Australian Government through the
846 Education Investment Fund and the Department of Industry and Science, in partnership with
847 Western Sydney University.
848

849 **Table 1.** Hypothesized plant processes and ecosystem state variables affecting pre-drought
850 resistance and post-drought recovery in the context of unprecedented climate extremes (UCEs).
851 The “Included in Model?” column indicates which processes or state variables are represented in
852 each of the two models studied in this paper. The mechanisms listed in the two right columns
853 refer to real-world ecosystems and are not necessarily represented in the ED2 and LPJ-GUESS
854 models. Contents of the table are based on a non-exhaustive literature review, expert knowledge,
855 and modeling results presented here. Symbols refer to the following literature sources: *
856 Borchert et al., 2002; Williams et al., (2008); ** Dietze and Matthes, (2014); O’Brien et al.,
857 2014; *** ENQUIST and ENQUIST, (2011); Greenwood et al., (2017); Powell et al., (2018); ^
858 Rowland et al., (2015); McDowell et al., (2013); Anderegg et al., (2015); ^^ Joslin et al., 2000;
859 Markewitz et al., (2010); ^^^ Powell et al., (2018); ^^^^ Bennett et al., (2015); Rowland et al.,
860 (2015); ~ Hubbard et al., (2013); ~ ~ McDowell et al., (2006); D’Amato et al., (2013); + Zhu et
861 al., (2018); Vargas et al., (2021); % Trugman et al., (2019); %% Franklin et al., (2012); %%
862 Franklin et al., (2020).

Process or State Variable	Included in model?	Mechanisms affecting pre-UCE drought resistance influencing impact	Mechanisms affecting post-UCE drought recovery
Processes			
1) Phenology Schemes	ED2: Yes LPJ-G: Yes	- Leaf area and metabolic activity modulates vulnerability to death - Drought-deciduousness reduces vulnerability to drought *, with higher water potential at turgor loss point and less leaf vulnerability to embolism +	- Leaf lifespan tends to increase from pioneer to late-successional species in some ecosystems (e.g., tropical forests) and is a balance between C gain and its cost
2) Plant Hydraulics	ED2: Yes LPJ-G: No	- Cavitation resistance traits ^ - Turgor loss, hydraulic failure (stem embolism) lead to increased plant mortality and enhanced vulnerability to secondary stressors.	- Replacement cost of damaged xylem slows recovery of surviving trees
3) Dynamic Carbon Allocation	ED2: Yes LPJ-G: Yes	- Increased root allocation could offset soil water deficit under gradual onset of drought ^^ - Leaf C allocation strategies should be connected to hydraulic processes %	- Allocation among fine roots, xylem, & leaves affects recovery time & GPP/LAI trajectory - Eco-evolutionary optimality theory %%

4) Non-Structural Carbohydrate (NSC) Storage	ED2: Yes LPJ-G: Yes	- NSCs buffer C starvation mortality due to reduced primary productivity. - Maintenance of hydraulic function & avoiding hydraulic failure **	- Low NSC could increase vulnerability to secondary stressors during recovery
State Variables			
1) Plant-Soil Water Availability	ED2: Yes LPJ-G: Partly	- Low soil water potential increases risk of tree C starvation, turgor loss and hydraulic failure	- After stand dieback reduced demand for soil resources &/or reduced shading - Increased soil water enhances regeneration/ regrowth, buffers vulnerability to long-term drought ~ ~
2) Plant Functional Diversity	ED2: Yes LPJ-G: Yes	- Presence of drought-tolerant species modulates resistance at community level. - Shallow-rooting species more vulnerable ^^ ^***	- Changed resource spectra shift competitive balance in favor of grasses and pioneer trees
3) Stand Demography	ED2: Yes LPJ-G: Yes	- Larger tree size enhances vulnerability to drought and secondary stressors due to higher maintenance costs ^^ ^^	- Mortality of canopy individuals favors understory species and smaller size-classes - Self-organizing principles %%%
4) Compounding Stressors	ED2: No LPJ-G: No	- Reduced resistance to insects and pathogens due to physiological/mechanical/ hydraulic damage & depletion of NSC	- Infestation by insects and pathogens, repair of damage due to secondary stressors, slows recovery of surviving trees ~

864 **Table 2** Impact of eCO₂ and/or temperature on the integrated-C-change (kg C m⁻² yr) relative to
865 drought treatments with no additional warming or eCO₂, for both models, and both sites seen in
866 Fig. 3. Quantified as average and minimum integrated-C-change across all 20 drought intensities
867 for step-change scenarios of warming and eCO₂. The percentage of each scenario that was
868 negative in integrated-C-change (i.e., decreases in C loss). Green values represent positive
869 integrated-C-change.

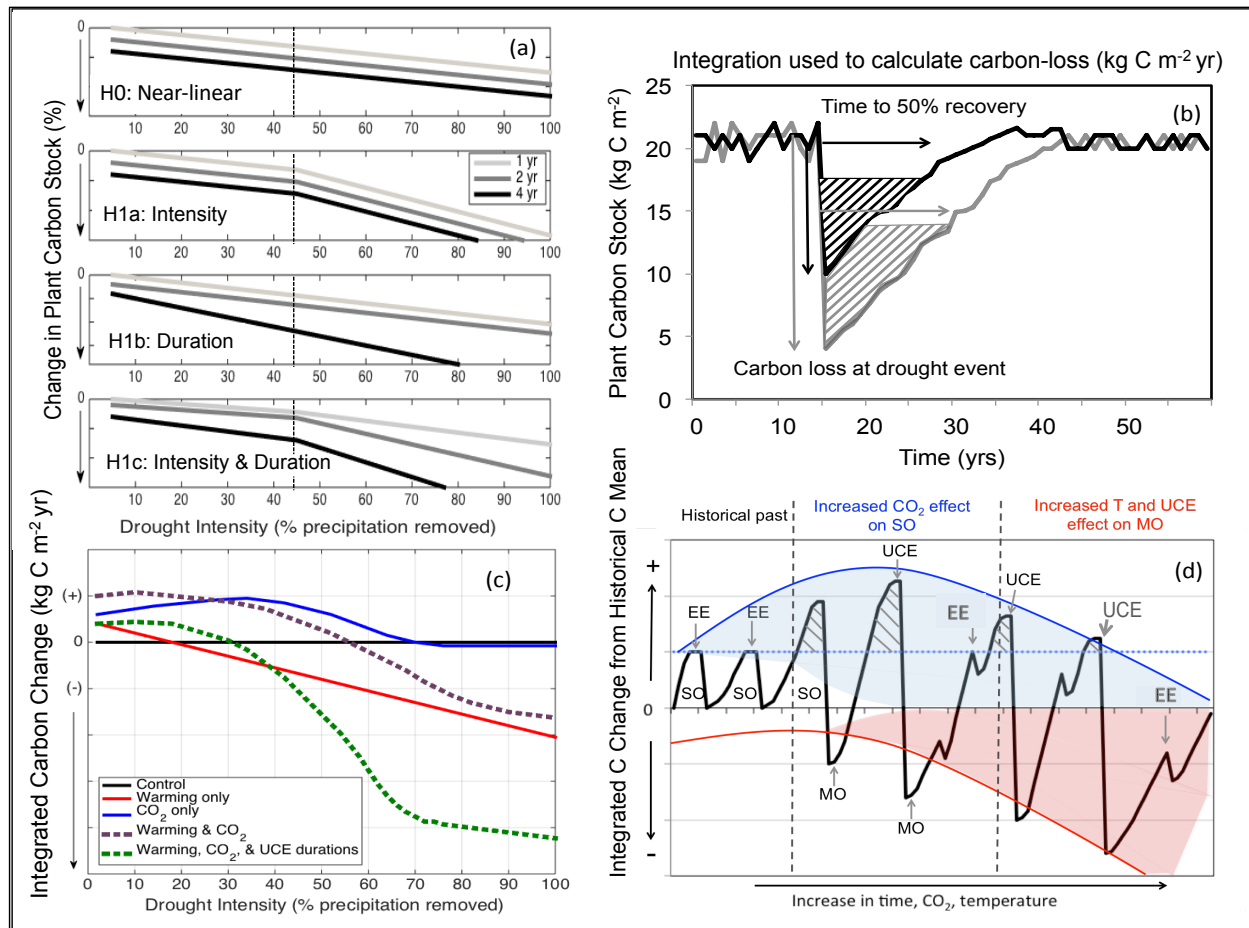
<i>EucFACE</i>	<i>ED2</i>			<i>LPJ-GUESS</i>			
	Average integrated C change	Largest integrated C change	% climate scenario was negative	Average integrated C change	Largest integrated C change	% climate scenario was negative	
1 year	600 ppm	2.2	0.0	33.3	-74.6	-396.6	36.8
	800 ppm	-10.6	-73.0	50.0	-124.1	-416.0	57.9
	2K	2.3	-0.5	16.7	21.3	-20.8	15.8
	2K, 600 ppm	0.5	-8.2	61.1	-67.5	-201.5	78.9
	2K, 800 ppm	1.8	-0.4	22.2	-145.9	-400.1	47.4
2 year	600 ppm	-105.6	-456.7	77.8	-85.2	-260.6	63.2
	800 ppm	-199.0	-522.9	83.3	-106.3	-350.1	42.1
	2K	-10.3	-34.7	77.8	14.2	-35.2	31.6
	2K, 600 ppm	-204.9	-666.1	77.8	-47.6	-128.8	84.2
	2K, 800 ppm	-12.4	-61.6	50.0	-167.0	-421.9	68.4
4 year	600 ppm	-125.5	-306.2	83.3	-122.6	-277.4	94.7
	800 ppm	-277.1	-423.3	100.0	-212.2	-523.7	89.5
	2K	-61.8	-188.6	72.2	12.9	-13.8	31.6
	2K, 600 ppm	-385.9	-674.2	94.4	-79.1	-197.3	94.7
	2K, 800 ppm	-277.9	-737.7	72.2	-247.0	-503.8	100.0
Average	-111.0	-277.0	64.8	-95.4	-276.5	62.5	
<i>Palo Verde</i>	<i>ED2</i>			<i>LPJ-GUESS</i>			
1 year	600 ppm	-1.6	-6.2	77.8	-11.0	-32.4	78.9
	800 ppm	6.7	-0.2	11.1	-39.2	-154.0	100.0
	2K	-1.0	-15.3	38.9	-33.4	-75.1	100.0
	2K, 600 ppm	2.5	-1.1	22.2	6.5	-4.6	52.6
	2K, 800 ppm	-6.6	-16.6	77.8	-121.1	-237.7	100.0
2 year	600 ppm	15.1	-16.7	38.9	27.3	-6.0	10.5
	800 ppm	-229.2	-756.6	66.7	20.6	-17.2	26.3
	2K	-8.2	-71.8	50.0	32.0	-12.7	15.8
	2K, 600 ppm	24.8	-5.7	11.1	36.2	-1.2	5.3
	2K, 800 ppm	-152.9	-348.1	77.8	8.0	-54.5	36.8
4 year	600 ppm	-11.1	-37.3	94.4	3.4	-25.1	26.3
	800 ppm	-260.2	-694.8	94.4	-25.2	-132.6	57.9
	2K	-39.0	-133.8	66.7	-7.7	-45.9	68.4
	2K, 600 ppm	1.0	-16.4	38.9	6.1	-4.1	31.6
	2K, 800 ppm	-148.5	-429.3	83.3	-20.0	-75.5	78.9
Average	-53.9	-170.0	56.7	-7.8	-58.6	52.6	

870

871 **Table 3** Summary of suggested critical look of driving mechanisms (e.g., ecosystem or plant
 872 processes and state variables) which emerged from the hypothetical drought simulations used
 873 here to explore for future research in manipulation experiments, data collection, and model
 874 development and testing, as related to furthering our understanding of UCE resistance and
 875 recovery.

UCE Drought Resistance & Recovery Summary	
Processes	Suggestions of driving mechanisms to further explore in data and models
1) Phenology Schemes	Represent morphological and physiological traits relevant to plant-water relations; drought- deciduousness can reduce vulnerability to drought; phenology of evergreens needs more investigation.
2) Plant Hydraulics	Interactions between hydraulic failure (e.g. low soil moisture availability) and C limitation (e.g. stomatal closure) during drought should be included in models. Account for turgor loss, hydraulic failure traits, costs to recover damaged xylem.
3) Dynamic Carbon Allocation	C allocation based on eco-evolutionary optimality (EEO) and allometric partitioning theory in addition, or replacing ratio-based optimal partitioning theory, and fixed ratios. Explore root allocation that could offset soil water deficits.
4) Non-structural Carbohydrate (NSC) Storage	Deciding best practices for NSC representation in models. Better understanding of NSC storage required to mitigate plant mortality during C starvation and interactions with avoiding hydraulic failure during severe droughts.
States Variables	
1) Plant-Soil Water Availability	Better quantification of the amount and accessibility of plant-available water for surviving trees, and tradeoff between increased structural productivity but vulnerability to subsequent droughts. Future relevance, or benefit, of lower water demand due to thinning with UCEs.
2) Plant Functional Diversity	Understand how higher diversity of plant physiological traits and drought-resistance strategies will enhance community resistance to drought; models still need to account for shifts in diverse functionality, including deciduousness shifts and interplay of regrowth structural overshoot followed by amplified mortality from hotter UCEs.
3) Stand Demography	Large trees more vulnerable to drought; need data on changes in C stock with UCEs in high-density smaller tree stands vs. stands with larger trees. Using ‘self-organization’ principles for modeling stand level competition and coexistence under UCEs.

876

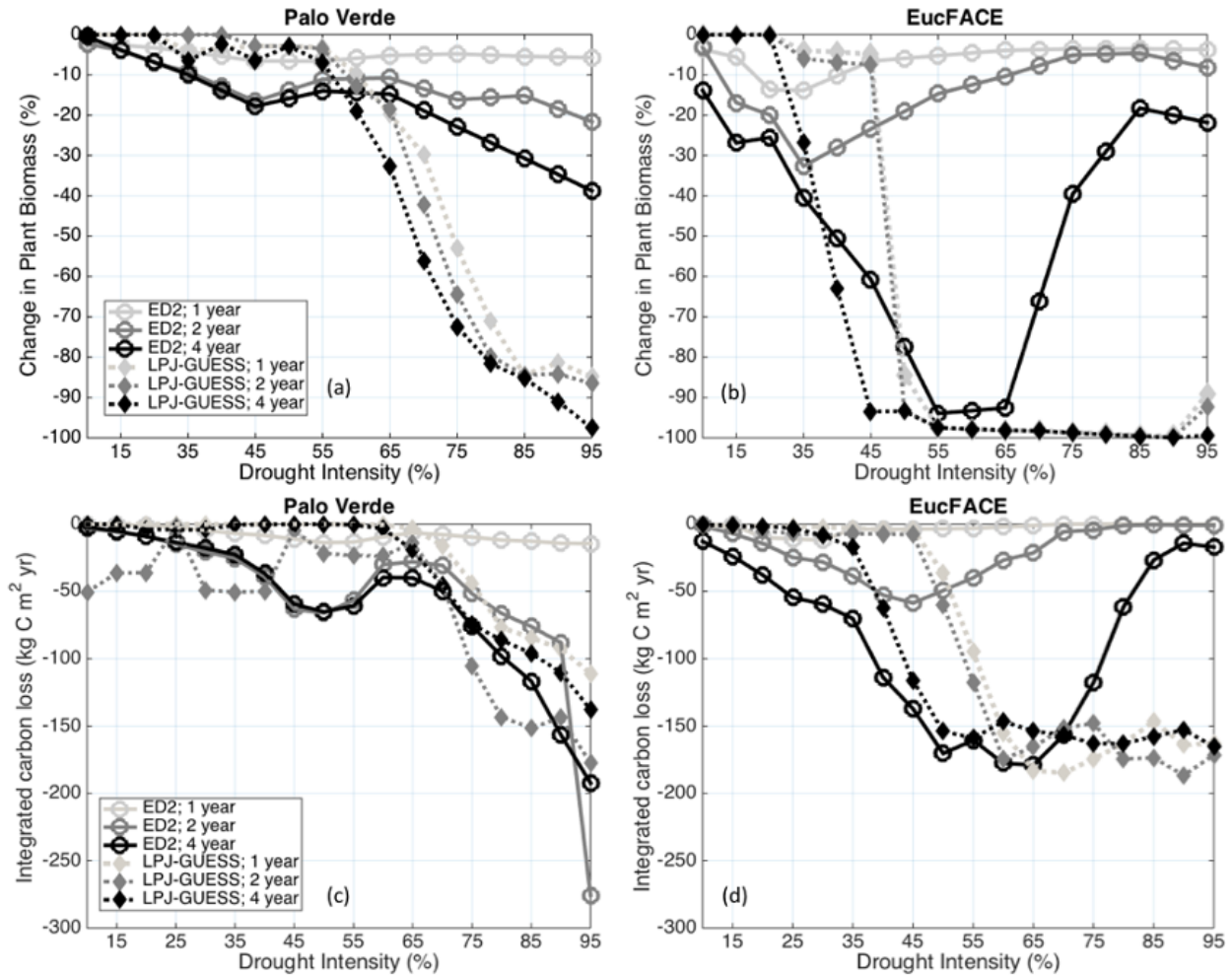


878

879 **Figure 1** Conceptual diagrams showing impacts of extreme droughts (unprecedented climate
 880 extremes, UCEs; i.e., record-breaking droughts) on plant C stocks. (a) **Conceptual response**
 881 **diagram**: potential loss in C stock as a function of increasing drought intensity (0-100%
 882 precipitation removal) and drought duration (1, 2 or 4 years of drought). In this example, an
 883 arbitrary threshold of 45% precipitation reduction and 4-year drought duration is assumed to
 884 correspond to a UCE. The “null hypothesis” (H0, top panel) is a near-linear response of C stocks
 885 to droughts. Alternative hypotheses include nonlinear and threshold responses to drought
 886 intensity (H1a), drought duration via different slope responses (H1b), and combined effects of
 887 both drought intensity and durations (H1c). (b) **Conceptualized UCE C loss diagram**:
 888 responses of forest C stocks to a large (grey) and small (black) UCE. “Integrated-C-loss” (kg C
 889 m⁻² yr) denotes the integral of the C loss over time and is calculated from the two arrows: the
 890 total loss in C (kg C m⁻²) due to drought, and the time (yr) to recover 50% of the pre-drought C
 891 stock. (c) **Conceptualized UCE-climate C change diagram**: hypothetical response in terrestrial

892 “integrated-C-change” ($\text{kg C m}^{-2} \text{ yr}$) due to eCO_2 (blue line), rising temperature (red line),
893 interaction between eCO_2 and temperature (dashed purple), and combined interactions among
894 eCO_2 , temperature, and UCEs of prolonged durations (green line), all relative to a reference
895 drought of normal duration with no warming (black line). Integrated-C-change denotes the
896 difference in integrated-C-loss (see panel b) between a scenario of changing climatic drivers and
897 the reference drought (control). (d) **Conceptual UCE amplification diagram**: hypothetical
898 amplified change in forest C stocks to eCO_2 and temperature relative to the pre-warming
899 historical past (based on Jump et al. (2017)). Change in C stock greater than zero indicates a
900 ‘structural overshoot’ (SO) due to favorable environmental conditions and/or recovery from an
901 extreme drought-heat event (EE). Hashed black areas indicate a structural overshoot due to
902 eCO_2 , which occurs over the historical CO_2 levels (dashed blue line). Initially, an eCO_2 effect
903 leads to a larger increase in structural overshoot (due to CO_2 fertilization), driving more extreme
904 vegetation mortality (‘mortality overshoot’ - MO) relative to historical dieback events and thus a
905 greater decrease in C stock. Increased warming through time increasingly counteracts any CO_2
906 fertilization effect; while the amplitude of post-UCE C stock recoveries remains large, net C
907 stock values eventually decline (downward curvature) due to more pronounced loss in C stocks
908 (and greater ecosystem state change) from hotter UCEs.
909 SO = structural overshoot, MO = mortality overshoot, EE = historically extreme drought-heat
910 event, UCE = unprecedented climate extreme.

911

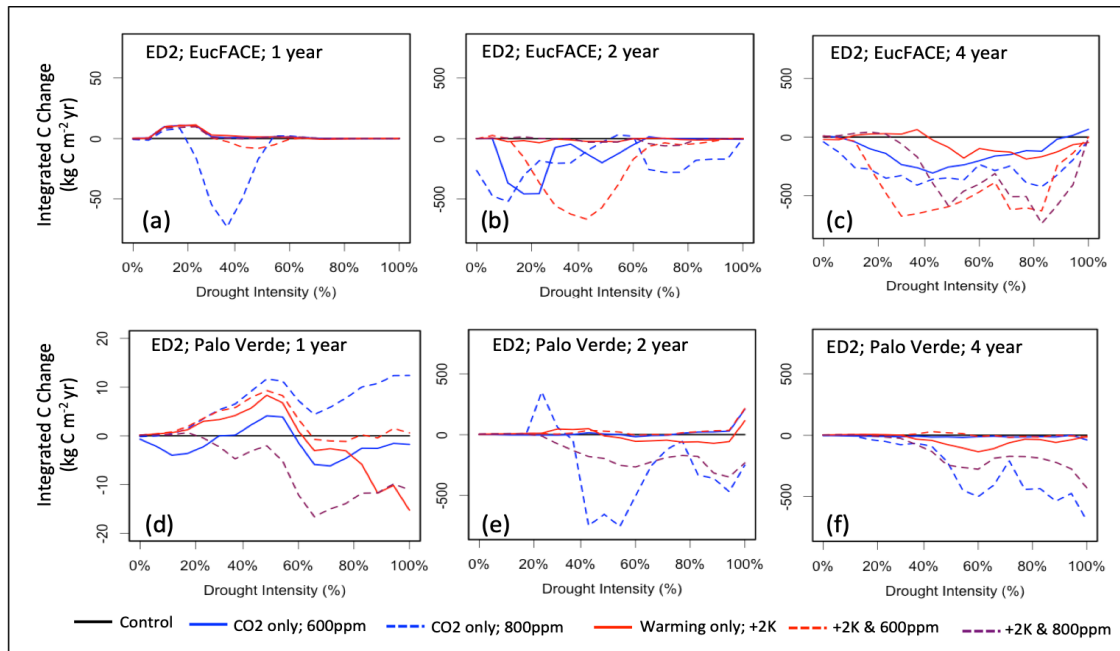


912

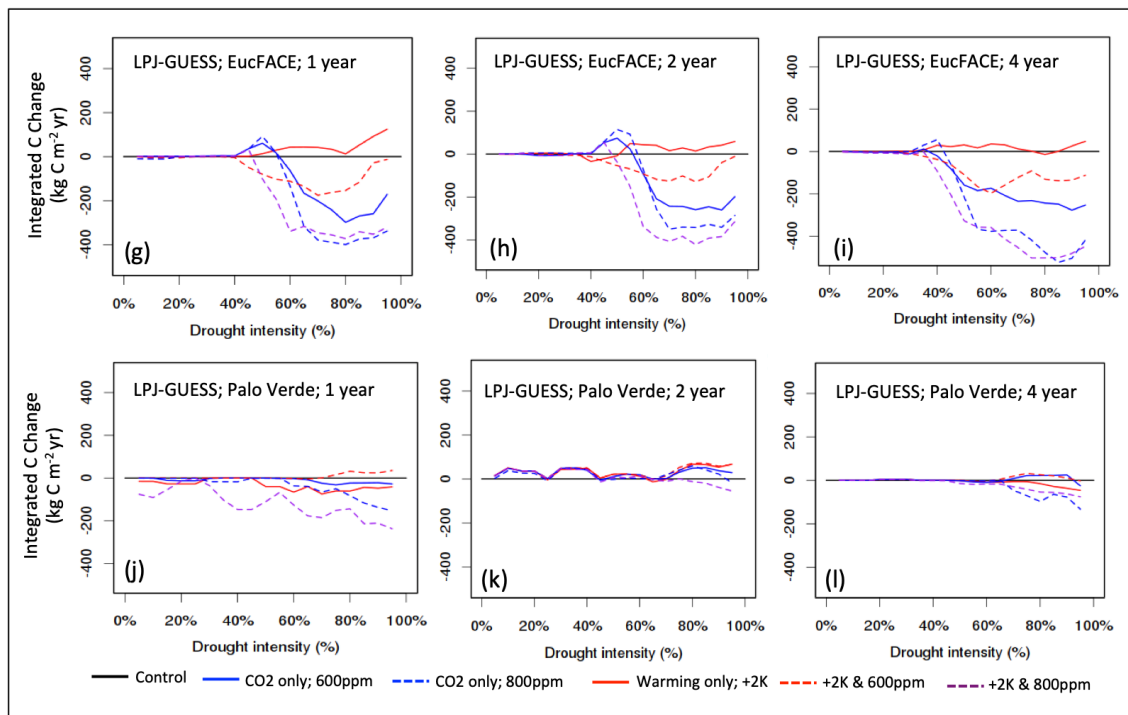
913 **Figure 2** Modeled change in biomass (%) at the end of drought periods of different lengths (1, 2,
 914 and 4-year droughts) and intensities (up to 95% precipitation removed) at (a) Palo Verde, and (b)
 915 EucFACE, for the ED2 and LPJ-GUESS models. Modeled integrated-C-loss (C reduction due to
 916 extreme drought integrated over time until biomass recovers to 50% of the non-drought baseline
 917 biomass) at (c) Palo Verde and (d) EucFACE.

918

919



920

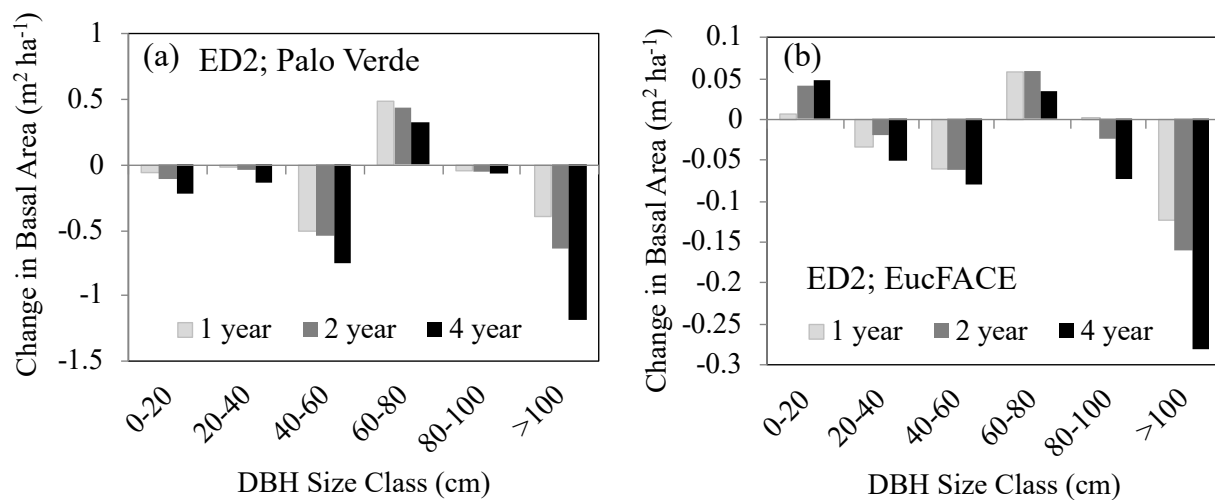


921 **Figure 3** Vegetation C response to interactions between drought intensity (0% to 100%
 922 precipitation reduction), drought durations (1, 2, 4-year droughts), and idealized scenarios of
 923 warming and eCO₂ compared to the reference simulation, simulated by two VDMs; ED2 (a-f)
 924 and LPJ-GUESS (g-l) at two sites (EucFACE and Palo Verde). The scenarios include a control
 925 (current temperature; 400 ppm atmospheric CO₂), two eCO₂ scenarios (600 ppm or 800 ppm),

926 elevated temperature (2 K above current), and a combination of eCO₂ (600 ppm or 800 ppm) and
 927 higher temperature. Vegetation response is quantified as “integrated-C-change” (in kg C m⁻² yr;
 928 Eq. 4), which is defined as the difference in integrated-C-losses due to drought between a given
 929 scenario of change in climatic drivers and the control. Negative values for integrated-C-change
 930 indicate that warming and/or eCO₂ leads to stronger C losses and/or longer recovery, while
 931 positive values for integrated-C-change indicates a buffering effect.

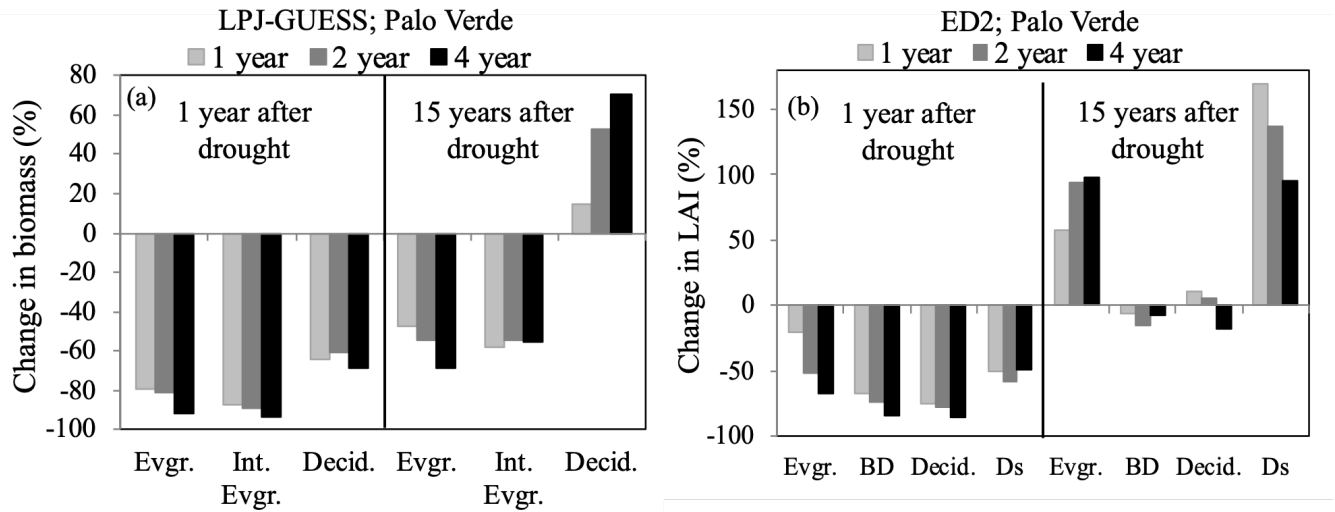
932

933



934

935 **Figure 4** Change in basal area (m² ha⁻¹) immediately following either 1, 2, or 4 year droughts for
 936 six increasing size class bins (DBH, cm) as predicted by the ED2 model for (a) the Palo Verde
 937 site, with 90% precipitation removed, and (b) the EucFACE site with 50% precipitation
 938 removed.



940

941

942 **Figure 5** Percent change in community composition, represented by plant functional type (PFT),

943 the year following three drought durations of UCEs (1, 2, and 4-year droughts and 90%

944 precipitation removed) as well as 15 years after droughts, for the tropical Palo Verde site by (a)

945 LPJ-GUESS reported in biomass change, and (b) ED2 reported in LAI change. Even though Ds

946 had the strongest recovery, it should be noted it was the least abundant PFT at this site. Evgr. =

947 evergreen, Int. Ever. = intermediate evergreen, Decid. = deciduous, BD = brevi-deciduous, Ds =

948 deciduous stem-succulent. EucFACE data not shown because only one PFT present (evergreen

949 tree).

950 References:

951

952 Adams, H.D., Guardiola-Claramonte, M., Barron-Gafford, G.A., Villegas, J.C., Breshears, D.D.,
953 Zou, C.B. et al.: Temperature sensitivity of drought-induced tree mortality portends
954 increased regional die-off under global-change-type drought, *PNAS*, 106, 7063-7066, 2009.

955 Adams, H.D., Barron-Gafford, G.A., Minor, R.L., Gardea, A.A., Bentley, L.P., Law, D.J. et al.:
956 Temperature response surfaces for mortality risk of tree species with future drought,
957 *Environ. Res. Lett.*, 12, 115014, 2017a.

958 Adams, H.D., Zeppel, M.J.B., Anderegg, W.R.L., Hartmann, H., Landhäusser, S.M., Tissue, D.T.
959 et al.: A multi-species synthesis of physiological mechanisms in drought-induced tree
960 mortality, *Nature Ecol. & Evol.*, 1, 1285-1291, 2017b.

961 Aguirre, BA, Hsieh, B, Watson, SJ, Wright, AJ.: The experimental manipulation of atmospheric
962 drought: Teasing out the role of microclimate in biodiversity experiments, *J. Ecol.*, 109,
963 1986– 1999, <https://doi.org/10.1111/1365-2745.13595>, 2021.

964 Ahlström, A., Schurgers, G., Arneeth, A., and Smith, B.: Robustness and uncertainty in terrestrial
965 ecosystem carbon response to CMIP5 climate change projections, *Environ. Res. Lett.*, 7,
966 044008, 2012.

967 Ainsworth, E.A., and Long, S.P.: What have we learned from 15 years of free-air CO₂
968 enrichment (FACE)? A meta-analytic review of the responses of photosynthesis, canopy
969 properties and plant production to rising CO₂, *New Phytol.*, 165, 351-372, 2005.

970 Allen, C.D., Breshears, D.D., and McDowell, N.G.: On underestimation of global vulnerability to
971 tree mortality and forest die-off from hotter drought in the Anthropocene, *Ecosphere*, 6,
972 art129, 2015.

973 Allen, K., Dupuy, J.M., Gei, M.G., Hulshof, C.M., Medvigy, D., Pizano, C. et al.: Will seasonally
974 dry tropical forests be sensitive or resistant to future changes in 558 rainfall regimes?
975 *Environ. Res. Lett.*, 12, 023001, 2017.

976 Amiro, B.D., Barr, A.G., Barr, J.G., Black, T.A., Bracho, R., Brown, M. et al.: Ecosystem carbon
977 dioxide fluxes after disturbance in forests of North America, *J. Geophys. Res.*
978 *Biogeosciences*, 115, 2010.

979 Anderegg, W.R.L., Hicke, J.A., Fisher, R.A., Allen, C.D., Aukema, J., Bentz, B. et al.: Tree
980 mortality from drought, insects, and their interactions in a changing climate, *New Phytol.*,
981 208, 674-683, 2015.

982 Anderegg, W.R.L., Klein, T., Bartlett, M., Sack, L., Pellegrini, A.F.A., Choat, B. et al.: Meta-
983 analysis reveals that hydraulic traits explain cross-species patterns of drought-induced tree
984 mortality across the globe, *PNAS*, 113, 5024-5029, 2016a.

985 Anderegg, W.R.L., Martinez-Vilalta, J., Cailleret, M., Camarero, J.J., Ewers, B.E., Galbraith, D.
986 et al.: When a Tree Dies in the Forest: Scaling Climate-Driven Tree Mortality to Ecosystem
987 Water and Carbon Fluxes, *Ecosystems*, 19, 1133-1147, 2016b.

988 Anderegg, W.R.L., Konings, A.G., Trugman, A.T., Yu, K., Bowling, D.R., Gabbitas, R. et al.:
989 Hydraulic diversity of forests regulates ecosystem resilience during drought, *Nature*, 561,
990 538-541, 2018.

991 Anderegg, W.R.L. and Venturas, M.D.: Plant hydraulics play a critical role in Earth system
992 fluxes, *New Phytol*, 226, 1535-1538, <https://doi.org/10.1111/nph.16548>, 2020.

993 Asner, G.P., Brodrick, P.G., Anderson, C.B., Vaughn, N., Knapp, D.E., and Martin, R.E.:
994 Progressive forest canopy water loss during the 2012–2015 California drought. *PNAS*, 113,
995 E249-E255, 2016.

996 Arora, V.K., Katavouta, A., Williams, R.G., Jones, C.D., Brovkin, V., Friedlingstein, P., et al.:
997 Carbon-concentration and carbon-climate feedbacks in CMIP6 models and their
998 comparison to CMIP5 models, *Biogeosciences*, 17, 4173–4222, 2020.

999 Bai, Y., Wu, J., Xing, Q., Pan, Q., Huang, J., Yang, D. et al.: PRIMARY PRODUCTION AND
1000 RAIN USE EFFICIENCY ACROSS A PRECIPITATION GRADIENT ON THE
1001 MONGOLIA PLATEAU, *Ecology*, 89, 2140-2153, 2008.

1002 Beier, C., Beierkuhnlein, C., Wohlgemuth, T., Penuelas, J., Emmett, B., Körner, C. et al.:
1003 Precipitation manipulation experiments – challenges and recommendations for the future,
1004 *Ecol. Lett.*, 15, 899-911, 2012.

1005 Bennett, A.C., McDowell, N.G., Allen, C.D., and Anderson-Teixeira, K.J.: Larger trees suffer
1006 most during drought in forests worldwide, *Nature Plants*, 1, 15139, 2015.

1007 Biederman, J.A., Meixner, T., Harpold, A.A., Reed, D.E., Gutmann, E.D., Gaun, J.A. et al.:
1008 Riparian zones attenuate nitrogen loss following bark beetle-induced lodgepole pine
1009 mortality, *J. Geophys. Res. Biogeosciences*, 121, 933-948, 2016.

1010 Biederman, J.A., Somor, A.J., Harpold, A.A., Gutmann, E.D., Breshears, D.D., Troch, P.A. et al.:
1011 Recent tree die-off has little effect on streamflow in contrast to expected increases from
1012 historical studies, *Water Resources Res.*, 51, 9775-9789, 2015.

1013 Blyth, E.M., Arora, V.K., Clark, D.B. et al.: Advances in Land Surface Modelling, *Curr. Clim.*
1014 *Change Rep.*, 7, 45–71, <https://doi.org/10.1007/s40641-021-00171-5>, 2021.

1015 Borchert, R., Rivera, G., and Hagnauer, W.: Modification of Vegetative Phenology in a Tropical
1016 Semi-deciduous Forest by Abnormal Drought and Rain, *Biotropica*, 34, 27-39, 2002.

1017 Bonan, G.: Vegetation Demography, in: *Climate Change and Terrestrial Ecosystem Modeling*,
1018 Cambridge: Cambridge University Press, 344-364, doi:10.1017/9781107339217.020, 2019.

1019 Bonan, G. B., Patton, E. G., Finnigan, J. J., Baldocchi, D. D., and Harman, I. N.: Moving beyond
1020 the incorrect but useful paradigm: reevaluating big-leaf and multilayer plant canopies to
1021 model biosphere-atmosphere fluxes – a review, *Agr. Forest Meteorol.*, 306,
1022 108435, <https://doi.org/10.1016/j.agrformet.2021.108435>, 2021.

1023 Brando, P.M., Paolucci, L., Ummenhofer, C.C., Ordway, E.M., Hartmann, H., Cattau, M.E.,
1024 Rattis, L., Medjibe, V., Coe, M.T., Balch, J.: Droughts, Wildfires, and Forest Carbon
1025 Cycling: A Pantropical Synthesis, *Annual Review of Earth and Planetary Sciences*, 47, 555-
1026 581, 2019.

1027 Breshears, D.D., Myers, O.B., Meyer, C.W., Barnes, F.J., Zou, C.B., Allen, C.D. et al.: Tree die-
1028 off in response to global change-type drought: mortality insights from a decade of plant
1029 water potential measurements, *Front. Ecol. Environ.*, 7, 185-189, 2009.

1030 Brodribb, T.J., Bowman, D.J.M.S., Nichols, S., Delzon, S. and Burlett, R.: Xylem function and
1031 growth rate interact to determine recovery rates after exposure to extreme water deficit, *New*
1032 *Phytol.*, 188, 533-542, 2010.

1033 Bugmann, H., and Seidl, R.: The evolution, complexity and diversity of models of long-term
1034 forest dynamics. *J. of Ecol.*, 110, 2288– 2307, <https://doi.org/10.1111/1365-2745.13989>,
1035 2022.

1036 Carreño-Rocabado, G., Peña-Claros, M., Bongers, F., Alarcón, A., Licona, J.-C., and Poorter, L.:
1037 Effects of disturbance intensity on species and functional diversity in a tropical forest, *J.*
1038 *Ecology*, 100, 1453-1463, 2012.

1039 Chapman, T.B., Veblen, T.T., and Schoennagel, T.: Spatiotemporal patterns of mountain pine
1040 beetle activity in the southern Rocky Mountains, *Ecology*, 93, 2175-2185, 2012.

1041 Chiang, F., Mazdiyasn, O., and AghaKouchak, A.: Evidence of anthropogenic impacts on global
1042 drought frequency, duration, and intensity, *Nat Commun.*, 12, 2754,
1043 <https://doi.org/10.1038/s41467-021-22314-w>, 2021.

1044 Choat, B., Brodribb, T.J., Brodersen, C.R., Duursma, R.A., López, R., and Medlyn, B.E.: Triggers
1045 of tree mortality under drought, *Nature*, 558, 531-539, 2018.

1046 Choat, B., Jansen, S., Brodribb, T.J., Cochard, H., Delzon, S., Bhaskar, R. et al.: Global
1047 convergence in the vulnerability of forests to drought, *Nature*, 491, 752-755, 2012.

1048 Christoffersen, B.O., Gloor, M., Fauset, S., Fyllas, N.M., Galbraith, D.R., Baker, T.R. et al.:
1049 Linking hydraulic traits to tropical forest function in a size-structured and trait-driven model
1050 (TFS v.1-Hydro), *Geosci. Model Dev. Discuss.*, 2016, 1-60, 2016.

1051 Ciais, P., Reichstein, M., Viovy, N., Granier, A., Ogée, J., Allard, V. et al.: Europe-wide
1052 reduction in primary productivity caused by the heat and drought in 2003, *Nature*, 437, 529,
1053 2005.

1054 Ciais, P., Sabine, C., Bala, G., Bopp, L., Brovkin, V., Canadell, J., et al.: Carbon and other
1055 biogeochemical cycles. In: *Climate Change 2013: The Physical Science Basis. Contribution of Working Group I to the Fifth Assessment Report of the*
1056 *Intergovernmental Panel on Climate Change* (eds. Stocker, T.F., Qin, D., Plattner, G.-K.,
1057 Tignor, M., Allen, S.K., Boschung, J., et al.), Cambridge University Press, Cambridge,
1058 United Kingdom and New York, NY, USA, pp. 465–570, 2013.

1060 Clark, K.L., Skowronski, N., and Hom, J.: Invasive insects impact forest carbon dynamics, *Glob.*
1061 *Change Biol.*, 16, 88-101, 2010.

1062 Coley, P., Massa, M., Lovelock, C., Winter, K.: Effects of elevated CO₂ on foliar chemistry of
1063 saplings of nine species of tropical tree, *Oecologia*, 2002.

1064 Creeden, E.P., Hicke, J.A., and Buotte, P.C.: Climate, weather, and recent mountain pine beetle
1065 outbreaks in the western United States, *Forest Ecol. Manag.*, 312, 239-251, 2014.

1066 D'Amato, A.W., Bradford, J.B., Fraver, S. and Palik, B.J.: Effects of thinning on drought
1067 vulnerability and climate response in north temperate forest ecosystems, *Eco. Applications*,
1068 23, 1735-1742, 2013.

1069 da Costa, A.C.L., Galbraith, D., Almeida, S., Portela, B.T.T., da Costa, M., de Athaydes Silva
1070 Junior, J. et al., Effect of 7 yr of experimental drought on vegetation dynamics and biomass
1071 storage of an eastern Amazonian rainforest, *New Phytol.*, 187, 579-591, 2010.

1072 De Kauwe, M.G., Medlyn, B.E., Zaehle, S., Walker, A.P., Dietze, M.C., Wang, Y.-P. et al.:
1073 Where does the carbon go? A model-data intercomparison of vegetation carbon allocation
1074 and turnover processes at two temperate forest free-air CO₂ enrichment sites, *New Phytol*,
1075 203, 883-899, 2014.

1076 Dietze, M.C., and Matthes, J.H.: A general ecophysiological framework for modelling the impact
1077 of pests and pathogens on forest ecosystems, *Ecol. Lett.*, 17, 1418-1426, 2014.

1078 Döscher, R., Acosta, M., et al.: The EC-Earth3 Earth System Model for the Climate Model
1079 Intercomparison Project 6, *Geosci. Model Dev. Discuss.* [preprint],
1080 <https://doi.org/10.5194/gmd-2020-446>, in revision, 2022.

1081 Dreesen, F.E., De Boeck, H.J., Janssens, I.A., and Nijs, I.: Do successive climate extremes
1082 weaken the resistance of plant communities? An experimental study using plant
1083 assemblages, *Biogeosciences*, 11, 109-121, 2014.

1084 Duursma, R.A., Gimeno, T.E., Boer, M.M., Crous, K.Y., Tjoelker, M.G. and Ellsworth, D.S.:
1085 Canopy leaf area of a mature evergreen *Eucalyptus* woodland does not respond to elevated

1086 atmospheric [CO₂] but tracks water availability, *Glob. Change Biol.*, 22, 1666-
1087 1676, <https://doi.org/10.1111/gcb.13151>, 2016.

1088 Eamus, D., Boulain, N., Cleverly, J., and Breshears, D.D.: Global change-type drought-induced
1089 tree mortality: vapor pressure deficit is more important than temperature per se in causing
1090 decline in tree health, *Ecol. Evol.*, 3, 2711-2729, 2013.

1091 Eller, C.B., Rowland, L., Mencuccini, M., Rosas, T., Williams, K., Harper, A. et al.: Stomatal
1092 optimization based on xylem hydraulics (SOX) improves land surface model simulation of
1093 vegetation responses to climate, *New Phytol.*, 226, 1622-
1094 1637, <https://doi.org/10.1111/nph.16419>, 2020.

1095 Ellsworth, David S., Anderson, Ian C., Crous, Kristine Y., Cooke, J., Drake, John E., Gherlenda,
1096 Andrew N. et al.: Elevated CO₂ does not increase eucalypt forest productivity on a low-
1097 phosphorus soil, *Nature Climate Change*, 7, 279, 2017.

1098 ENQUIST, B.J., and ENQUIST, C.A.F.: Long-term change within a Neotropical forest: assessing
1099 differential functional and floristic responses to disturbance and drought, *Glob. Change*
1100 *Biol.*, 17, 1408-1424, 2011.

1101 Esquivel-Muelbert, A., Baker, T.R., Dexter, K.G., Lewis, S.L., Brienen, R.J.W., Feldpausch, T.R.
1102 et al.: Compositional response of Amazon forests to climate change, *Glob. Change Biol.*, 25,
1103 39-56, 2019.

1104 Eziz, A., Yan, Z., Tian, D., Han, W., Tang, Z., and Fang, J.: Drought effect on plant biomass
1105 allocation: A meta-analysis, *Ecol. Evol.*, 7, 11002-11010, 2017.

1106 Fang, Y., Leung, L. R., Knox, R., Koven, C., and Bond-Lamberty, B.: Impact of the numerical
1107 solution approach of a plant hydrodynamic model (v0.1) on vegetation dynamics, *Geosci.*
1108 *Model Dev.*, 15, 6385–6398, <https://doi.org/10.5194/gmd-15-6385-2022>, 2022.

1109 Feldpausch, T.R., Phillips, O.L., Brienen, R.J.W., Gloor, E., Lloyd, J., Lopez-Gonzalez, G. et al.:
1110 Amazon forest response to repeated droughts, *Global Biogeochemical Cycles*, 30, 964-982,
1111 2016.

1112 Fisher, R.A., Muszala, S., Versteinstein, M., Lawrence, P., Xu, C., McDowell, N.G. et al.: Taking
1113 off the training wheels: the properties of a dynamic vegetation model without climate
1114 envelopes, *CLM4.5(ED)*, *Geosci. Model Dev.*, 8, 3593-3619, 2015.

1115 Fisher, R.A., Koven, C.D., Anderegg, W.R.L., Christoffersen, B.O., Dietze, M.C., Farrior, C.E. et
1116 al.: Vegetation demographics in Earth System Models: A review of progress and priorities,
1117 *Glob. Change Biol.*, 24, 35-54, 2018.

1118 Fisher, R. A., and Koven, C. D.: Perspectives on the future of land surface models and the
1119 challenges of representing complex terrestrial systems, *JAMES*, 12,
1120 e2018MS001453, <https://doi.org/10.1029/2018MS001453>, 2020.

1121 Fleischer, K., Rammig, A., De Kauwe, M.G., Walker, A.P., Domingues, T.F., Fuchslueger, L. et
1122 al.: Amazon forest response to CO₂ fertilization dependent on plant phosphorus acquisition,
1123 *Nature Geoscience*, 12, 736-741, 2019.

1124 Frank, D., Reichstein, M., Bahn, M., Thonicke, K., Frank, D., Mahecha, M.D. et al.: Effects of
1125 climate extremes on the terrestrial carbon cycle: concepts, processes and potential future
1126 impacts, *Glob. Change Biol.*, 21, 2861-2880, 2015.

1127 Franklin, O., McMurtrie, R.E., Iversen, C.M., Crous, K.Y., Finzi, A.C., Tissue, D.T., Ellsworth,
1128 D.S., Oren, R. Norby, R.J.: Forest fine-root production and nitrogen use under elevated
1129 CO₂: contrasting responses in evergreen and deciduous trees explained by a common
1130 principle, *Glob. Change Biol.*, 15, 132-144, 2009.

- 1131 Franklin, O., Johansson, J., Dewar, R.C., Dieckmann, U., McMurtrie, R.E., Brännström, Å.,
 1132 Dybzinski, R.: Modeling carbon allocation in trees: a search for principles, *Tree Physiology*,
 1133 32, 648–666, <https://doi.org/10.1093/treephys/tpr138>, 2012.
- 1134 Franklin, O., Harrison, S.P., Dewar, R. et al.: Organizing principles for vegetation dynamics. *Nat.*
 1135 *Plants*, 6, 444–453, <https://doi.org/10.1038/s41477-020-0655-x>, 2020.
- 1136 Friend, A.D., Lucht, W., Rademacher, T.T., Keribin, R., Betts, R., Cadule, P. et al.: Carbon
 1137 residence time dominates uncertainty in terrestrial vegetation responses to future climate
 1138 and atmospheric CO₂, *PNAS*, 111, 3280–3285, 2014.
- 1139 Gerten, D., LUO, Y., Le MAIRE, G., PARTON, W.J., KEOUGH, C., WENG, E. et al.: Modelled
 1140 effects of precipitation on ecosystem carbon and water dynamics in different climatic zones,
 1141 *Glob. Change Biol.*, 14, 2365–2379, 2008.
- 1142 Goulden, M.L., and Bales, R.C.: California forest die-off linked to multi-year deep soil drying in
 1143 2012–2015 drought, *Nature Geoscience*, 12, 632–637, 2019.
- 1144 Gray, S.B., Dermody, O., Klein, S.P., Locke, A.M., McGrath, J.M., Paul, R.E. et al.: Intensifying
 1145 drought eliminates the expected benefits of elevated carbon dioxide for soybean, *Nature*
 1146 *Plants*, 2, 16132, 2016.
- 1147 Greenwood, S., Ruiz-Benito, P., Martínez-Vilalta, J., Lloret, F., Kitzberger, T., Allen, C.D. et al.:
 1148 Tree mortality across biomes is promoted by drought intensity, lower wood density and
 1149 higher specific leaf area, *Ecol. Lett.*, 20, 539–553, 2017.
- 1150 Griffin, D., and Anchukaitis, K.J.: How unusual is the 2012–2014 California drought? *Geophys.*
 1151 *Res. Lett.*, 41, 9017–9023, 2014.
- 1152 Hanbury-Brown, A.R., Powell, T.L., Muller-Landau, H.C., Wright, S.J. and Kueppers, L.M.:
 1153 Simulating environmentally-sensitive tree recruitment in vegetation demographic models,
 1154 *New Phytol.*, 235, 78–93, <https://doi.org/10.1111/nph.18059>, 2022.
- 1155 Harrison, S.P., Cramer, W., Franklin, O., Prentice, I.C., Wang, H., Brännström, Å., et al.: Eco-
 1156 evolutionary optimality as a means to improve vegetation and land-surface models, *New*
 1157 *Phytol.*, 231, 2125–2141, <https://doi.org/10.1111/nph.17558>, 2021.
- 1158 Hickler, T., Smith, B., Sykes, M.T., Davis, M.B., Sugita, S., and Walker, K.: USING A
 1159 GENERALIZED VEGETATION MODEL TO SIMULATE VEGETATION DYNAMICS
 1160 IN NORTHEASTERN USA, *Ecology*, 85, 519–530, 2004.
- 1161 Holm, J. A., Knox, R. G., Zhu, Q., Fisher, R. A., Koven, C. D., Nogueira Lima, A. J., et al.: The
 1162 central Amazon biomass sink under current and future atmospheric CO₂: Predictions from
 1163 big-leaf and demographic vegetation models, *J. Geophys. Res. Biogeosciences*, 125,
 1164 e2019JG005500. <https://doi.org/10.1029/2019JG005500>, 2020.
- 1165 Hovenden, M.J., Newton, P.C.D., and Wills, K.E.: Seasonal not annual rainfall determines
 1166 grassland biomass response to carbon dioxide, *Nature*, 511, 583, 2014.
- 1167 Hubbard, R.M., Rhoades, C.C., Elder, K., and Negron, J.: Changes in transpiration and foliage
 1168 growth in lodgepole pine trees following mountain pine beetle attack and mechanical
 1169 girdling, *Forest Ecol. Manag.*, 289, 312–317, 2013.
- 1170 IPCC: Managing the Risks of Extreme Events and Disasters to Advance Climate Change
 1171 Adaptation. A Special Report of Working Groups I and II of the Intergovernmental Panel on
 1172 Climate Change. (ed. Field, C.B., V. Barros, T.F. Stocker, D. Qin, D.J. Dokken, K.L. Ebi,
 1173 M.D. Mastrandrea, K.J. Mach, G.-K. Plattner, S.K. Allen, M. Tignor, and P.M. Midgley)
 1174 Cambridge, UK, and New York, NY, USA, p. 582 pp, 2012.
- 1175 IPCC: Climate Change 2021: The Physical Science Basis. Contribution of Working Group I to the
 1176 Sixth Assessment Report of the Intergovernmental Panel on Climate Change [Masson-

1177 Delmotte, V., P. Zhai, A. Pirani, S.L. Connors, C. Péan, S. Berger, N. Caud, Y. Chen, L.
1178 Goldfarb, M.I. Gomis, M. Huang, K. Leitzell, E. Lonnoy, J.B.R. Matthews, T.K. Maycock,
1179 T. Waterfield, O. Yelekçi, R. Yu, and B. Zhou (eds.)]. Cambridge University Press, 2021.

1180 Jiang, M., Medlyn, B.E., Drake, J.E., Duursma, R.A., Anderson, I.C., Barton, C.V.M., Boer,
1181 M.B., Carrillo, Y., Castañeda-Gómez, L., Collins, L., et al.: The fate of carbon in a mature
1182 forest under carbon dioxide enrichment, *Nature*, 580, 227-231,
1183 <https://doi.org/10.1038/s41586-020-2128-9>, 2020.

1184 Joslin, J.D., Wolfe, M.H., and Hanson, P.J.: Effects of altered water regimes on forest root
1185 systems, *New Phytol.*, 147, 117-129, 2000.

1186 Jump, A.S., Ruiz-Benito, P., Greenwood, S., Allen, C.D., Kitzberger, T., Fensham, R. et al.:
1187 Structural overshoot of tree growth with climate variability and the global spectrum of
1188 drought-induced forest dieback, *Glob. Change Biol.*, 23, 3742-3757, 2017.

1189 Kalacska, M.E.R., Sánchez-Azofeifa, G.A., Calvo-Alvarado, J.C., Rivard, B. and Quesada, M.:
1190 Effects of Season and Successional Stage on Leaf Area Index and Spectral Vegetation
1191 Indices in Three Mesoamerican Tropical Dry Forests, *Biotropica*, 37, 486-
1192 496, <https://doi.org/10.1111/j.1744-7429.2005.00067.x>, 2005.

1193 Kannenberg, S.A., Schwalm, C.R. and Anderegg, W.R.L.: Ghosts of the past: how drought legacy
1194 effects shape forest functioning and carbon cycling, *Ecol. Lett.*, 23: 891-901,
1195 <https://doi.org/10.1111/ele.13485>, 2020.

1196 Kattge, J., DÍAZ, S., LAVOREL, S., PRENTICE, I.C., LEADLEY, P., BÖNISCH, G. et al.: TRY
1197 – a global database of plant traits, *Global Change Biol*, 17, 2905-2935, 2011.

1198 Kayler, Z.E., De Boeck, H.J., Fatichi, S., Grünzweig, J.M., Merbold, L., Beier, C. et al.:
1199 Experiments to confront the environmental extremes of climate change, *Front. Ecol.*
1200 *Environ.*, 13, 219-225, 2015.

1201 Keenan, T.F., Hollinger, D.Y., Bohrer, G., Dragoni, D., Munger, J.W., Schmid, H.P. et al.:
1202 Increase in forest water-use efficiency as atmospheric carbon dioxide concentrations rise,
1203 *Nature*, 499, 324-327, 2013.

1204 Kennedy, D., Swenson, S., Oleson, K. W., Lawrence, D. M., Fisher, R., Lola da Costa, A. C., and
1205 Gentine, P.: Implementing plant hydraulics in the Community Land Model, version 5,
1206 *JAMES*, 11, 485– 513, <https://doi.org/10.1029/2018MS001500>, 2019.

1207 Li, L., Yang, Z.-L., Matheny, A. M., Zheng, H., Swenson, S. C., Lawrence, D. M., et
1208 al.: Representation of plant hydraulics in the Noah-MP land surface model: Model
1209 development and multiscale evaluation, *JAMES*, 13,
1210 e2020MS002214, <https://doi.org/10.1029/2020MS002214>, 2021.

1211 Li, Q., Lu, X., Wang, Y., Huang, X., Cox, P. M., and Luo, Y.: Leaf area index identified as a
1212 major source of variability in modeled CO₂ fertilization, *Biogeosciences*, 15, 6909–6925,
1213 <https://doi.org/10.5194/bg-15-6909-2018>, 2018.

1214 Liu, Y., Parolari, A.J., Kumar, M., Huang, C.-W., Katul, G.G., and Porporato, A.: Increasing
1215 atmospheric humidity and CO₂ concentration alleviate forest mortality risk, *PNAS*, 114,
1216 9918-9923, 2017.

1217 Lloret, F., Escudero, A., Iriondo, J.M., Martínez-Vilalta, J., and Valladares, F.: Extreme climatic
1218 events and vegetation: the role of stabilizing processes, *Glob. Change Biol.*, 18, 797-805,
1219 2012.

1220 Luo, Y., Gerten, D., Le Maire, G., Parton, W.J., Weng, E., Zhou, X. et al.: Modeled interactive
1221 effects of precipitation, temperature, and [CO₂] on ecosystem carbon and water dynamics in
1222 different climatic zones, *Glob. Change Biol.*, 14, 1986-1999, 2008.

1223 Luo, Y.Q., Randerson, J.T., Abramowitz, G., Bacour, C., Blyth, E., Carvalhais, N. et al.: A
1224 framework for benchmarking land models, *Biogeosciences*, 9, 3857-3874, 2012.

1225 Luo, Y., Jiang, L., Niu, S., Zhou, X.: Nonlinear responses of land ecosystems to variation in
1226 precipitation, *New Phytol.*, 214, 5–7, 2017.

1227 Ma, W., Zhai, L., Pivovarov, A., Shuman, J., Buotte, P., Ding, J., Christoffersen, B., Knox, R.,
1228 Moritz, M., Fisher, R. A., Koven, C. D., Kueppers, L., and Xu, C.: Assessing climate
1229 change impacts on live fuel moisture and wildfire risk using a hydrodynamic vegetation
1230 model, *Biogeosciences*, 18, 4005–4020, <https://doi.org/10.5194/bg-18-4005-2021>, 2021.

1231 MacGillivray, C.W., Grime, J.P., and The Integrated Screening Programme, T.: Testing
1232 Predictions of the Resistance and Resilience of Vegetation Subjected to Extreme Events,
1233 *Funct. Ecol.*, 9, 640-649, 1995.

1234 Markewitz, D., Devine, S., Davidson, E.A., Brando, P., and Nepstad, D.C.: Soil moisture
1235 depletion under simulated drought in the Amazon: impacts on deep root uptake, *New
1236 Phytol.*, 187, 592-607, 2010.

1237 Matusick, G., Ruthrof, K.X., Brouwers, N.C., Dell, B., and Hardy, G.S.J.: Sudden forest canopy
1238 collapse corresponding with extreme drought and heat in a mediterranean-type eucalypt
1239 forest in southwestern Australia, *European J. Forest Res.*, 132, 497-510, 2013.

1240 Matusick, G., Ruthrof, K.X., Fontaine, J.B., and Hardy, G.E.S.J.: Eucalyptus forest shows low
1241 structural resistance and resilience to climate change-type drought, *J. Vegetation Science*,
1242 27, 493-503, 2016.

1243 McCarthy, M.C., and Enquist, B.J.: Consistency between an allometric approach and optimal
1244 partitioning theory in global patterns of plant biomass allocation, *Funct. Ecol.*, 21, 713-720,
1245 2007.

1246 McDowell, N., Pockman, W.T., Allen, C.D., Breshears, D.D., Cobb, N., Kolb, T. et al.:
1247 Mechanisms of plant survival and mortality during drought: why do some plants survive
1248 while others succumb to drought? *New Phytol.*, 178, 719-739, 2008.

1249 McDowell, N.G., Adams, H.D., Bailey, J.D., Hess, M., and Kolb, T.E.: Homeostatic Maintenance
1250 Of Ponderosa Pine Gas Exchange In Response To Stand Density Changes, *Ecological
1251 Applications*, 16, 1164-1182, 2006.

1252 McDowell, N.G., and Allen, C.D.: Darcy's law predicts widespread forest mortality under climate
1253 warming, *Nature Climate Change*, 5, 669-672, 2015.

1254 McDowell, N.G., Beerling, D.J., Breshears, D.D., Fisher, R.A., Raffa, K.F., and Stitt, M.: The
1255 interdependence of mechanisms underlying climate-driven vegetation mortality, *Trends in
1256 Ecol. & Evolution*, 26, 523-532, 2011.

1257 McDowell, N.G., Fisher, R.A., Xu, C., Domec, J.C., Hölttä, T., Mackay, D.S. et al.: Evaluating
1258 theories of drought-induced vegetation mortality using a multimodel–experiment
1259 framework, *New Phytol.*, 200, 304-321, 2013.

1260 Medlyn, B.E., De Kauwe, M.G., Zaehle, S., Walker, A.P., Duursma, R.A., Luus, K., Mishurov,
1261 M., Pak, B., Smith, B., Wang, Y.-P., Yang, X., Crous, K.Y., Drake, J.E., Gimeno, T.E.,
1262 Macdonald, C.A., Norby, R.J., Power, S.A., Tjoelker, M.G. and Ellsworth, D.S.: Using
1263 models to guide field experiments: a priori predictions for the CO₂ response of a nutrient-
1264 and water-limited native Eucalypt woodland, *Glob. Change Biol.*, 22, 2834-2851, 2016.

1265 Medvigy, D., Wang, G., Zhu, Q., Riley, W.J., Trierweiler, A.M., Waring, B., Xu, X. and Powers,
1266 J.S.: Observed variation in soil properties can drive large variation in modelled forest
1267 functioning and composition during tropical forest secondary succession, *New Phytol*, 223,
1268 1820-1833, <https://doi.org/10.1111/nph.15848>, 2019.

- 1269 Medvigy, D., Clark, K.L., Skowronski, N.S., and Schäfer, K.V.R.: Simulated impacts of insect
1270 defoliation on forest carbon dynamics, *Environ. Res. Lett.*, 7, 045703, 2012.
- 1271 Medvigy, D. and Moorcroft, P.R.: Predicting ecosystem dynamics at regional scales: an
1272 evaluation of a terrestrial biosphere model for the forests of northeastern North America,
1273 *Philosophical Transactions of the Royal Society B: Biological Sciences*, 367, 222-235,
1274 2012.
- 1275 Medvigy, D., Wofsy, S., Munger, J., Hollinger, D. and Moorcroft, P.: Mechanistic scaling of
1276 ecosystem function and dynamics in space and time: Ecosystem Demography model version
1277 2, *J. Geophys. Res. Biogeosciences*, 114, 2009.
- 1278 Mencuccini, M., Manzoni, S., and Christoffersen, B.: Modelling water fluxes in plants: from
1279 tissues to biosphere, *New Phytol.*, 222, 1207-1222, <https://doi.org/10.1111/nph.15681>, 2019.
- 1280 Meir, P., Wood, T.E., Galbraith, D.R., Brando, P.M., Da Costa, A.C.L., Rowland, L. et al.:
1281 Threshold Responses to Soil Moisture Deficit by Trees and Soil in Tropical Rain Forests:
1282 Insights from Field Experiments, *BioScience*, 65, 882-892, 2015.
- 1283 Montané, F., Fox, A.M., Arellano, A.F., MacBean, N., Alexander, M.R., Dye, A. et al.:
1284 Evaluating the effect of alternative carbon allocation schemes in a land surface model
1285 (CLM4.5) on carbon fluxes, pools, and turnover in temperate forests, *Geosci. Model Dev.*,
1286 10, 3499-3517, 2017.
- 1287 Muldavin, E.H., Moore, D.I., Collins, S.L., Wetherill, K.R., and Lightfoot, D.C.: Aboveground
1288 net primary production dynamics in a northern Chihuahuan Desert ecosystem, *Oecologia*,
1289 155, 123-132, 2008.
- 1290 Myers, J.A., and Kitajima, K.: Carbohydrate storage enhances seedling shade and stress tolerance
1291 in a neotropical forest, *J. Ecology*, 95, 383-395, 2007.
- 1292 Niklas, K. J.: The scaling of plant height: A comparison among major plant clades and anatomical
1293 grades, *Annals of Botany*, 72, 165-172, <https://doi.org/10.1006/anbo.1993.1095>, 1993.
- 1294 Norby, R.J., DeLucia, E.H., Gielen, B., Calfapietra, C., Giardina, C.P., King, J.S. et al.: Forest
1295 response to elevated CO₂ is conserved across a broad range of productivity, *PNAS*, 102,
1296 18052-18056, 2005.
- 1297 O'Brien, M.J., Leuzinger, S., Philipson, C.D., Tay, J., and Hector, A.: Drought survival of
1298 tropical tree seedlings enhanced by non-structural carbohydrate levels, *Nature Climate
1299 Change*, 4, 710, 2014.
- 1300 Obermeier, W.A., Lehnert, L.W., Kammann, C.I., Müller, C., Grünhage, L., Luterbacher, J. et al.:
1301 Reduced CO₂ fertilization effect in temperate C₃ grasslands under more extreme weather
1302 conditions, *Nature Climate Change*, 7, 137, 2016.
- 1303 Palace, M., Keller, M., and Silva, H.: NECROMASS PRODUCTION: STUDIES IN
1304 UNDISTURBED AND LOGGED AMAZON FORESTS, *Ecological Applications*, 18, 873-
1305 884, 2008.
- 1306 Petit, G., Anfodillo, T., Mencuccini, M.: Tapering of xylem conduits and hydraulic limitations in
1307 sycamore (*Acer pseudoplatanus*) trees, *New Phytol.*, 177, 653-
1308 664. <https://doi.org/10.1111/j.1469-8137.2007.02291.x>, 2008.
- 1309 Phillips, O.L., Aragão, L.E.O.C., Lewis, S.L., Fisher, J.B., Lloyd, J., López-González, G. et al.:
1310 Drought Sensitivity of the Amazon Rainforest, *Science*, 323, 1344-1347, 2009.
- 1311 Phillips, O.L., van der Heijden, G., Lewis, S.L., López-González, G., Aragão, L.E.O.C., Lloyd, J.
1312 et al.: Drought-mortality relationships for tropical forests, *New Phytol.*, 187, 631-646, 2010.
- 1313 Pilon, C.E., Côté, B., and Fyles, J.W.: Effect of an artificially induced drought on leaf peroxidase
1314 activity, mineral nutrition and growth of sugar maple, *Plant and Soil*, 179, 151-158, 1996.

1315 Potter, C., Klooster, S., Hiatt, C., Genovese, V., and Castilla-Rubio, J.C.: Changes in the carbon
1316 cycle of Amazon ecosystems during the 2010 drought, *Environ. Res. Lett.*, 6, 034024, 2011.

1317 Powell, T.L., Galbraith, D.R., Christoffersen, B.O., Harper, A., Imbuzeiro, H.M.A., Rowland, L.
1318 et al.: Confronting model predictions of carbon fluxes with measurements of Amazon
1319 forests subjected to experimental drought, *New Phytol.*, 200, 350-365, 2013.

1320 Powell, T.L., Koven, C.D., Johnson, D.J., Faybishenko, B., Fisher, R.A., Knox, Ryan G. et al.:
1321 Variation in hydroclimate sustains tropical forest biomass and promotes functional diversity,
1322 *New Phytol.*, 219, 932-946, 2018.

1323 Powers, J.S., Becknell, J.M., Irving, J., and Pérez-Aviles, D.: Diversity and structure of
1324 regenerating tropical dry forests in Costa Rica: Geographic patterns and environmental
1325 drivers, *Forest Ecol. Manag.*, 258, 959-970, 2009.

1326 Powers, J.S., and Pérez-Aviles, D.: Edaphic Factors are a More Important Control on Surface
1327 Fine Roots than Stand Age in Secondary Tropical Dry Forests, *Biotropica*, 45, 1-9, 2013.

1328 Powers, JS, Vargas G., G, Brodrribb, TJ, et al.: A catastrophic tropical drought kills hydraulically
1329 vulnerable tree species, *Glob. Change Biol.* 2020; 26: 3122– 3133,
1330 <https://doi.org/10.1111/gcb.15037>, 2020.

1331 Pugh, T.A.M., Rademacher, T., Shafer, S. L., Steinkamp, J., Barichivich, J., Beckage, B. et al.:
1332 Understanding the uncertainty in global forest carbon turnover, *Biogeosciences*, 17, 3961–
1333 3989, <https://doi.org/10.5194/bg-17-3961-2020>, 2020.

1334 Rapparini, F., and Peñuelas, J.: Mycorrhizal Fungi to Alleviate Drought Stress on Plant Growth.
1335 In: *Use of Microbes for the Alleviation of Soil Stresses*, Volume 1 (ed. Miransari, M),
1336 Springer New York New York, NY, pp. 21-42, 2014.

1337 Reich, P.B., Hobbie, S.E., and Lee, T.D.: Plant growth enhancement by elevated CO₂ eliminated
1338 by joint water and nitrogen limitation, *Nature Geoscience*, 7, 920, 2014.

1339 Reich, P.B., Wright, I.J., and Lusk, C.H.: PREDICTING LEAF PHYSIOLOGY FROM SIMPLE
1340 PLANT AND CLIMATE ATTRIBUTES: A GLOBAL GLOPNET ANALYSIS, *Ecological*
1341 *Applications*, 17, 1982-1988, 2007.

1342 Reichstein, M., Bahn, M., Ciais, P., Frank, D., Mahecha, M.D., Seneviratne, S.I. et al.: Climate
1343 extremes and the carbon cycle, *Nature*, 500, 287-295, 2013.

1344 Reyes, J.J., Tague, C.L., Evans, R.D., and Adam, J.C.: Assessing the Impact of Parameter
1345 Uncertainty on Modeling Grass Biomass Using a Hybrid Carbon Allocation Strategy, 9,
1346 2968-2992, 2017.

1347 Richardson, A.D., Carbone, M.S., Keenan, T.F., Czimczik, C.I., Hollinger, D.Y., Murakami, P. et
1348 al.: Seasonal dynamics and age of stemwood nonstructural carbohydrates in temperate forest
1349 trees, *New Phytol.*, 197, 850-861, 2013.

1350 Rowland, L., da Costa, A.C.L., Galbraith, D.R., Oliveira, R.S., Binks, O.J., Oliveira, A.A.R. et
1351 al.: Death from drought in tropical forests is triggered by hydraulics not carbon starvation,
1352 *Nature*, 528, 119, 2015.

1353 Roy, J., Picon-Cochard, C., Augusti, A., Benot, M.-L., Thiery, L., Darsonville, O. et al.: Elevated
1354 CO₂ maintains grassland net carbon uptake under a future heat and drought extreme, *PNAS*,
1355 113, 6224-6229, 2016.

1356 Ruppert, J.C., Harmony, K., Henkin, Z., Snyman, H.A., Sternberg, M., Willms, W. et al.:
1357 Quantifying drylands' drought resistance and recovery: the importance of drought intensity,
1358 dominant life history and grazing regime, *Glob. Change Biol.*, 21, 1258-1270, 2015.

1359 Rustad, L.E.: The response of terrestrial ecosystems to global climate change: Towards an
1360 integrated approach, *Science of The Total Environ.*, 404, 222-235, 2008.

1361 Ruthrof, K.X., Breshears, D.D., Fontaine, J.B., Froend, R.H., Matusick, G., Kala, J. et al.:
1362 Subcontinental heat wave triggers terrestrial and marine, multi-taxa responses, *Scientific*
1363 *Reports*, 8, 13094, 2018.

1364 Scheiter, S., Langan, L., and Higgins, S.I.: Next-generation dynamic global vegetation models:
1365 learning from community ecology, *New Phytol.*, 198, 957-969, 2013.

1366 Schenk, H.J., and Jackson, R.B.: Mapping the global distribution of deep roots in relation to
1367 climate and soil characteristics, *Geoderma*, 126, 129-140, 2005.

1368 Schwalm, C.R., Anderegg, W.R.L., Michalak, A.M., Fisher, J.B., Biondi, F., Koch, G. et al.:
1369 Global patterns of drought recovery, *Nature*, 548, 202, 2017.

1370 Seneviratne, S.I., X. Zhang, M. Adnan, W. Badi, C. Dereczynski, A. Di Luca, S. Ghosh, I.
1371 Iskandar, J. Kossin, S. Lewis, F. Otto, I. Pinto, M. Satoh, S.M. Vicente-Serrano, M. Wehner,
1372 and B. Zhou, 2021: Weather and Climate Extreme Events in a Changing Climate. In
1373 *Climate Change 2021: The Physical Science Basis. Contribution of Working Group I to the*
1374 *Sixth Assessment Report of the Intergovernmental Panel on Climate Change [Masson-*
1375 *Delmotte, V., P. Zhai, A. Pirani, S.L. Connors, C. Péan, S. Berger, N. Caud, Y. Chen, L.*
1376 *Goldfarb, M.I. Gomis, M. Huang, K. Leitzell, E. Lonnoy, J.B.R. Matthews, T.K. Maycock,*
1377 *T. Waterfield, O. Yelekçi, R. Yu, and B. Zhou (eds.)], Cambridge University Press,*
1378 *Cambridge, United Kingdom and New York, NY, USA, pp. 1513–1766,*
1379 *doi:10.1017/9781009157896.013, 2021.*

1380 Settele, J., Scholes, R., Betts, R., Bunn, S.E., Leadley, P., Nepstad, D., Overpeck, J.T., and
1381 Taboada, M.A.: Terrestrial and inland water systems. In: *Climate Change 2014: Impacts,*
1382 *Adaptation, and Vulnerability. Part A: Global and Sectoral Aspects. Contribution of*
1383 *Working Group II to the Fifth Assessment Report of the Intergovernmental Panel on*
1384 *Climate Change, Cambridge University Press Cambridge, United Kingdom and New York,*
1385 *NY, USA, pp. 271-359, 2014.*

1386 Sheffield, J., Goteti, G., and Wood, E.F.: Development of a 50-Year High-Resolution Global
1387 Dataset of Meteorological Forcings for Land Surface Modeling, *J. Climate*, 19, 3088-3111,
1388 2006.

1389 Shiels, A.B., Zimmerman, J.K., García-Montiel, D.C., Jonckheere, I., Holm, J., Horton, D. et al.:
1390 Plant responses to simulated hurricane impacts in a subtropical wet forest, Puerto Rico, *J.*
1391 *Ecology*, 98, 659-673, 2010.

1392 Silva, M., Matheny, A. M., Pauwels, V. R. N., Triadis, D., Missik, J. E., Bohrer, G., and Daly, E.:
1393 Tree hydrodynamic modelling of the soil–plant–atmosphere continuum using FETCH3,
1394 *Geosci. Model Dev.*, 15, 2619–2634, <https://doi.org/10.5194/gmd-15-2619-2022>, 2022.

1395 Sippel, S., Zscheischler, J., and Reichstein, M.: Ecosystem impacts of climate extremes crucially
1396 depend on the timing, *PNAS*, 113, 5768-5770, 2016.

1397 Sitch, S., HUNTINGFORD, C., GEDNEY, N., LEVY, P.E., LOMAS, M., PIAO, S.L. et al.:
1398 Evaluation of the terrestrial carbon cycle, future plant geography and climate-carbon cycle
1399 feedbacks using five Dynamic Global Vegetation Models (DGVMs), *Glob. Change Biol.*,
1400 14, 2015-2039, 2008.

1401 Skelton, R.P., West, A.G., and Dawson, T.E.: Predicting plant vulnerability to drought in
1402 biodiverse regions using functional traits, *PNAS*, 112, 5744-5749, 2015.

1403 Smith, B., Prentice, I.C., and Sykes, M.T.: Representation of vegetation dynamics in the
1404 modelling of terrestrial ecosystems: comparing two contrasting approaches within European
1405 climate space, *Global Ecol. Biogeo.*, 10, 621-637, 2001.

1406 Smith, B., Wårlind, D., Arneth, A., Hickler, T., Leadley, P., Siltberg, J. et al.: Implications of
1407 incorporating N cycling and N limitations on primary production in an individual-based
1408 dynamic vegetation model, *Biogeosciences*, 11, 2027-2054, 2014.

1409 Spasojevic, M.J., Bahlai, C.A., Bradley, B.A., Butterfield, B.J., Tuanmu, M.-N., Sistla, S. et al.:
1410 Scaling up the diversity–resilience relationship with trait databases and remote sensing data:
1411 the recovery of productivity after wildfire, *Glob. Change Biol.*, 22, 1421-1432, 2016.

1412 Sperry, J.S., Hacke, U.G., Oren, R., and Comstock, J.P.: Water deficits and hydraulic limits to
1413 leaf water supply, *Plant, Cell & Environ.*, 25, 251-263, 2002.

1414 Sperry, J.S., and Love, D.M.: What plant hydraulics can tell us about responses to climate-change
1415 droughts, *New Phytol.*, 207, 14-27, 2015.

1416 Sperry, J.S., Wang, Y., Wolfe, B.T., Mackay, D.S., Anderegg, W.R.L., McDowell, N.G. et al.:
1417 Pragmatic hydraulic theory predicts stomatal responses to climatic water deficits, *New*
1418 *Phytol.*, 212, 577-589, 2016.

1419 Stovall, A.E.L., Shugart, H., and Yang, X.: Tree height explains mortality risk during an intense
1420 drought, *Nature Communications*, 10, 4385, 2019.

1421 Tague, C.L., and Moritz, M.A.: Plant Accessible Water Storage Capacity and Tree-Scale Root
1422 Interactions Determine How Forest Density Reductions Alter Forest Water Use and
1423 Productivity, *Front. Forests and Global Change*, 2, 2019.

1424 Tomasella M, Petrusa E, Petruzzellis F, Nardini A, Casolo V.: The Possible Role of Non-
1425 Structural Carbohydrates in the Regulation of Tree Hydraulics, *International Journal of*
1426 *Molecular Sciences*, 21:144, <https://doi.org/10.3390/ijms21010144>, 2020.

1427 Trugman, A.T., Detto, M., Bartlett, M.K., Medvigy, D., Anderegg, W.R.L., Schwalm, C. et al.:
1428 Tree carbon allocation explains forest drought-kill and recovery patterns, *Ecol. Lett.*, 21,
1429 1552-1560, 2018.

1430 Trugman, A.T., Anderegg, L.D.L., Sperry, J.S., Wang, Y., Venturas, M., Anderegg,
1431 W.R.L.: Leveraging plant hydraulics to yield predictive and dynamic plant leaf allocation in
1432 vegetation models with climate change, *Glob. Change*
1433 *Biol.*, 25, 4008– 4021. <https://doi.org/10.1111/gcb.14814>, 2019.

1434 Uriarte, M., Lasky, J.R., Boukili, V.K., and Chazdon, R.L.: A trait-mediated, neighbourhood
1435 approach to quantify climate impacts on successional dynamics of tropical rainforests,
1436 *Funct. Ecol.*, 30, 157-167, 2016.

1437 Vargas G., G., Brodribb, T.J., Dupuy, J.M., González-M., R., Hulshof, C.M., Medvigy, D.,
1438 Allerton, T.A.P., Pizano, C., Salgado-Negret, B., Schwartz, N.B., Van Bloem, S.J., Waring,
1439 B.G. and Powers, J.S.: Beyond leaf habit: generalities in plant function across 97 tropical
1440 dry forest tree species, *New Phytol.*, 232: 148-161. <https://doi.org/10.1111/nph.17584>, 2021.

1441 Venturas, M. D., Todd, H. N., Trugman, A. T., and Anderegg, W. R.: Understanding and
1442 predicting forest mortality in the western United States using long-term forest inventory data
1443 and modeled hydraulic damage, *New Phytol.*, 230, 1896-1910, 2021.

1444 Wang, D., Heckathorn, S.A., Wang, X., and Philpott, S.M.: A meta-analysis of plant
1445 physiological and growth responses to temperature and elevated CO₂, *Oecologia*, 169, 1-13,
1446 2012.

1447 Weng, E.S., Malyshev, S., Lichstein, J.W., Farris, C.E., Dybzinski, R., Zhang, T. et al.: Scaling
1448 from individual trees to forests in an Earth system modeling framework using a
1449 mathematically tractable model of height-structured competition, *Biogeosciences*, 12, 2655-
1450 2694, 2015.

- 1451 Williams, A.P., Allen, C.D., Macalady, A.K., Griffin, D., Woodhouse, C.A., Meko, D.M. et al.:
1452 Temperature as a potent driver of regional forest drought stress and tree mortality, *Nature*
1453 *Climate Change*, 3, 292, 2012.
- 1454 Williams, A.P., Seager, R., Berkelhammer, M., Macalady, A.K., Crimmins, M.A., Swetnam,
1455 T.W. et al.: Causes and Implications of Extreme Atmospheric Moisture Demand during the
1456 Record-Breaking 2011 Wildfire Season in the Southwestern United States, *J. Applied*
1457 *Meteorology and Climatology*, 53, 2671-2684, 2014.
- 1458 Williams, L.J., Bunyavejchewin, S., and Baker, P.J.: Deciduousness in a seasonal tropical forest
1459 in western Thailand: interannual and intraspecific variation in timing, duration and
1460 environmental cues, *Oecologia*, 155, 571-582, 2008.
- 1461 Wullschleger, S.D., Hanson, P.J., and Todd, D.E.: Transpiration from a multi-species deciduous
1462 forest as estimated by xylem sap flow techniques, *For. Ecol. and Manage.*, 143, 205-213,
1463 2001.
- 1464 Xu, X., Medvigy, D., Powers, J.S., Becknell, J.M. and Guan, K.: Diversity in plant hydraulic
1465 traits explains seasonal and inter-annual variations of vegetation dynamics in seasonally dry
1466 tropical forests, *New Phytol.*, 212, 80-95, 2016.
- 1467 Yang, Y., Hillebrand, H., Lagisz, M., Cleasby, I., and Nakagawa, S.: Low statistical power and
1468 overestimated anthropogenic impacts, exacerbated by publication bias, dominate field
1469 studies in global change biology. *Glob. Change Biol.*, 28, 969– 989,
1470 <https://doi.org/10.1111/gcb.15972>, 2022.
- 1471 Zhu, K., Chiariello, N.R., Tobeck, T., Fukami, T., and Field, C.B.: Nonlinear, interacting
1472 responses to climate limit grassland production under global change, *PNAS*, 113, 10589-
1473 10594, 2016.
- 1474 Zhu, S-D., Chen, Y-J., Ye, Q., He, P-C., Liu, H., and Li, R-H., et al.: Leaf turgor loss point is
1475 correlated with drought tolerance and leaf carbon economics traits, *Tree Physiol.*, 38, 658–
1476 663, <https://doi.org/10.1093/treephys/tpy013>, 2018.
- 1477 Zscheischler, J., Mahecha, M.D., von Buttlar, J., Harmeling, S., Jung, M., Rammig, A. et al.: A
1478 few extreme events dominate global interannual variability in gross primary production,
1479 *Environ. Res. Lett.*, 9, 035001, 2014.